



Historical Biology

An International Journal of Paleobiology



ISSN: (Print) (Online) Journal homepage: <https://www.tandfonline.com/loi/ghbi20>

Plasticity in the morphology of the fused frontals of Albanerpetontidae (Lissamphibia; Allocaudata)

Alexandre R. D. Guillaume, Carlos Natário, Octávio Mateus & Miguel Moreno-Azanza

To cite this article: Alexandre R. D. Guillaume, Carlos Natário, Octávio Mateus & Miguel Moreno-Azanza (2022): Plasticity in the morphology of the fused frontals of Albanerpetontidae (Lissamphibia; Allocaudata), Historical Biology, DOI: [10.1080/08912963.2022.2054712](https://doi.org/10.1080/08912963.2022.2054712)

To link to this article: <https://doi.org/10.1080/08912963.2022.2054712>

 View supplementary material 

 Published online: 31 Mar 2022.

 Submit your article to this journal 

 Article views: 52

 View related articles 

 View Crossmark data 



Plasticity in the morphology of the fused frontals of Albanerpetontidae (Lissamphibia; Allocaudata)

Alexandre R. D. Guillaume ^{a,b}, Carlos Natário^a, Octávio Mateus ^{a,b} and Miguel Moreno-Azanza ^{a,b,c}

^aGEOBIOTEC, Department of Earth Sciences, NOVA School of Science and Technology, Campus de Caparica, P-2829 516 Caparica, Portugal; ^bMuseu da Lourinhã, Rua João Luís de Moura 95, 2530-158, Lourinhã, Portugal; ^cAragosaurus: Recursos Geológicos y Paleoambientes – IUCA. Departamento de Ciencias de la Tierra, Universidad de Zaragoza, España

ABSTRACT

Albanerpetontidae form an enigmatic extinct group of lissamphibians, ranging from the early Bathonian to the early Pleistocene. The Upper Jurassic outcrops of Portugal yield a large collection of material, suitable for addressing the intraspecific variation in and diagnostic potential of the characteristic fused frontals. We revise 58 specimens from the Guimarota beds of the Kimmeridgian Alcobaça Formation and describe 62 new frontal bones from the Kimmeridgian – Tithonian Lourinhã Formation. Smaller specimens exhibit a vermicular dorsal ornamentation, while it is polygonal in larger specimens and other albanerpetontids. Compared to small specimens, larger specimens display: (1) larger ventrolateral crests extending posteriorly after the parietal margin; (2) a relatively shorter internasal process; (3) a frontal width across posterior edges relatively smaller; and (4) a ventromedian crest less pronounced. Morphometric analyses suggest a single species with different ontogenetic stages. Specimens are attributed to aff. *Celtesdens* sp., based on a bell-shaped outline with a curved orbital margin (although variable in Portuguese specimens), and a flabellate, bulbous-shaped internasal process. The species is more similar to *C. megacephalus* than *C. ibericus*, but its phylogenetic position comprises an unresolved trichotomy. Our results show that intraspecific variation and homoplasy render the fused frontal non-diagnostic below the generic level.

ARTICLE HISTORY

Received 18 November 2021
Accepted 10 March 2022

KEYWORDS

Celtesdens; Guimarota beds; intraspecific variation; Lourinhã Formation; morphometry; phylogeny

Introduction

The Albanerpetontidae Fox and Naylor, 1982 form an extinct group of highly derived small amphibians characterised by: (1) fused frontals with polygonal dorsal ornamentation; (2) a ‘mortise and tenon’ interdentary joint; (3) distinctive non-pedicellate teeth with chisel-shaped, tricuspid crowns; and (4) two modified cervical vertebrae forming a tripartite facet similar to the atlas-axis complex in mammals (Gardner 2001; Gardner and Böhme 2008; Sweetman and Gardner 2013; Matsumoto and Evans 2018; Daza et al. 2020). Although they are considered as a distinct lineage (Fox and Naylor 1982; Gardner 2001), their position within crown Lissamphibia is still debated (Anderson 2008; Maddin et al. 2013; Matsumoto and Evans 2018; Marjanović and Laurin 2019; Daza et al. 2020). The albanerpetontid fossil record extends from the early Bathonian of France (Seiffert 1969), England (Evans and Milner 1994), and Morocco (Haddoumi et al. 2016), to the early Pleistocene of Italy (Villa et al. 2018). They were predominant in Laurasia (Gardner and Böhme 2008), although the material is scarce in Asia (Skutschas 2007; Matsumoto and Evans 2018; Daza et al. 2020), and specimens from Morocco are the only Gondwanian occurrences (Gardner et al. 2003; Haddoumi et al. 2016; Lasseron et al. 2020). The family Albanerpetontidae currently comprises six genera: the type genus *Albanerpeton* Estes and Hoffstetter, 1976 (Early Cretaceous – Pleistocene; Central Asia, Europe and North America); *Anoualerpeton* Gardner et al., 2003 (Bathonian – Berriasian; England and Morocco); *Celtesdens* McGowan and Evans, 1995 (Kimmeridgian – Albian; Europe); *Shirerpeton* Matsumoto and Evans, 2018 (Barremian; Japan); *Wesserpeton* Sweetman and

Gardner, 2013 (Barremian; England); and *Yaksha* Daza et al., 2020 (Cenomanian, Myanmar). However, the genus *Albanerpeton* as currently defined has been shown to be paraphyletic, although the authors did not review its taxonomy accordingly (Matsumoto and Evans 2018; Daza et al. 2020). Nevertheless, only Cenozoic species are now regarded as *Albanerpeton sensu stricto* (Daza et al. 2020).

The albanerpetontids are small animals and their fossil record is fragmentary and scarce, most are generally recovered as isolated bones by sieving sediments, with few exceptions. Articulated specimens with soft tissues preserved have been recovered from the Barremian Lagerstätte of Las Hoyas, in Spain (McGowan and Evans 1995; McGowan 2002; Evans 2016), the Albian Pietraroia bone bed in Italy (McGowan 2002), and from the early Cenomanian amber deposits of Myanmar, in which a complete articulated skull, a partial articulated post-cranial skeleton, and one juvenile specimen have been recorded (Daza et al. 2020). A handful of three-dimensional skulls in association have also been reported, from the Barremian of Japan (Matsumoto and Evans 2018) and the Pliocene of Hungary (Maddin et al. 2013).

Therefore, albanerpetontid taxonomy is mostly based on isolated but highly diagnostic bones (Gardner 2000a, 2001; Gardner et al. 2003; Gardner and Böhme 2008; Sweetman and Gardner 2013), among which fused frontals yield a relatively large set of diagnostic characters. The frontal bones have been thus considered to be key to both identifying and diagnosing taxa at the generic and specific level (McGowan 1998; Gardner 2000a). Most of the characters currently considered to be diagnostic for Albanerpetontidae are

confined to the skull, and the post-cranial skeleton is still poorly documented (Maddin et al. 2013). Previous phylogenetic analyses used seven characters relating to the frontal bones, of which: (1) an approximately triangular dorsal or ventral outline of the fused frontal has been considered as a synapomorphy of the clade (*Wesserpeton* + *Yaksha* + *Shirerpeton* + *Albanerpeton* s.l.); (2) a moderate ratio of midline length of fused frontals vs. width across posterior edge of bone, between lateral edges of ventrolateral crests, in large specimens has been considered as a synapomorphy of the clade *Albanerpeton* s.s.; (3) a bulbous dorsal or ventral outline of internasal process on frontals has been considered as a synapomorphy of *Celtedens*; (4) a long internasal process on fused frontals has been considered as a synapomorphy of the ‘robust-snouted’ clade (*Albanerpeton nexuosum* Estes 1981 + *Albanerpeton* s.s.), but is also recovered as an autapomorphy in *Anoualerpeton priscum* Gardner et al. 2003; (5) narrow and triangular ventrolateral crests on large, fused frontals in transverse view, with ventral face flat to shallowly concave was independently acquired in *An. priscum*, *Albanerpeton galaktion* Fox and Naylor 1982, and *A. nexuosum*; (6) wide and triangular ventrolateral crests on large, fused frontals in transverse view, with ventral face deeply concave has been independently acquired in *Albanerpeton inexpectatum* Estes and Hoffstetter 1976, and *Albanerpeton pannonicum* Venczel and Gardner 2005; and (7) the presence of a flattened ventromedial keel extending along posterior two-thirds of fused frontals has been independently acquired in *A. pannonicum* and *Shirerpeton isajii* Matsumoto and Evans 2018 (Gardner 2002; Gardner et al. 2003; Venczel and Gardner 2005; Sweetman and Gardner 2013; Matsumoto and Evans 2018; Daza et al. 2020).

The Portuguese albanerpetontid record in the Upper Jurassic is mainly known and represented by the Guimarães beds assemblage, from the Kimmeridgian Alcobaça Formation (Schudack 2000a). Thousands of specimens were recovered, making albanerpetontids as one of the commonest elements of the assemblage. Among these, more than 40 frontals were counted and attributed to a single new species of the genus *Celtedens* (Wiechmann 2000, 2003). Furthermore, the Lourinhã Formation, of late Kimmeridgian–Tithonian age (Mateus et al. 2017), also yields two localities: Porto Dinheiro (often misspelled Porto Pinheiro or Portinho), where hundreds of specimens were reported, including 16 frontals attributed to the same Alcobaça Fm. *Celtedens* species (Wiechmann 2003); and Porto das Barcas, where scarce material was referred to an undetermined albanerpetontid taxon, the lack of frontals and premaxillae precluding determination of its conspecificity or otherwise with other Portuguese material (Wiechmann 2003).

The Guimarães beds and the Lourinhã Fm. have important similarities concerning their faunal associations (Hahn and Hahn 2001; Martin 2001; Guillaume et al. 2020). Nevertheless, there is both a geographical (70 km) and, more importantly, a temporal gap (up to 5 million years) between both ecosystems. Furthermore, paleoenvironmental reconstructions of the Guimarães beds suggest a mangrove-like environment (Gloy 2000; Martin 2000), whereas the Lourinhã Fm. has been interpreted as a fluvial environment with marked seasonality (Martinius and Gowland 2011; Taylor et al. 2014; Gowland et al. 2017; Mateus et al. 2017). Thus, the presence of two different species, either successive species of a single lineage, or two contemporary species but niche-segregated, needs to be considered; especially when different but coeval species of albanerpetontids have been collected in different ages from the same localities (Gardner 2000b) or, in contrast, a single species occurred through a long period of time (Gardner et al. 2021). Being *a priori* diagnostic and one of the most abundant identifiable cranial elements found in Lourinhã and Guimarães collections, fused frontal bones are the potentially optimal specimens to test for the presence or absence of multiple taxa.

We here provide the description of new frontal material, although no specimen is complete. Intraspecific variation was examined to characterise the plasticity in the frontal bones, using linear morphometric analysis together with anatomical comparison. We are proposing an extended list of characters coded for all species and relevant specimens published.

Geological setting

The vertebrate microfossil assemblage (later referred as VMA) localities were sampled at outcrops at the top of cliffs in the municipality of Lourinhã, namely from South to North: Valmitão VMA, Zimbral VMA, and Porto das Barcas VMA (Figure 1). They occur within the Lourinhã Formation in the Lusitanian Basin, the largest sedimentary basin in Portugal (Wilson et al. 1989; Alves et al. 2003). The Lourinhã Fm. ranges from late Kimmeridgian to late Tithonian in age and lies between the Consolação unit and the Porto da Calada Formation (Taylor et al. 2014; Mateus et al. 2017). Its dominant continental deposits consist of sandy channel-fills and muddy floodplain deposits (Martinius and Gowland 2011; Taylor et al. 2014; Gowland et al. 2017), and it is comprised of three members: (1) the Kimmeridgian Porto Novo/Praia da Amoreira unit; (2) the late Kimmeridgian to early Tithonian Praia Azul member; and (3) the early Tithonian Santa Rita member (Taylor et al. 2014; Mateus et al. 2017).

The Valmitão VMA is located in the upper half of the Porto Novo/Praia da Amoreira unit and is distributed within a three-metre-thick mudstone layer with occasional intercalations of sandstones. Porto das Barcas, Porto Dinheiro, and Zimbral VMAs all belong to the Praia Azul member, the latter being younger and located on top of the Porto Dinheiro sequence previously sampled by the expedition of Institute of Geological Sciences, Freie Universität Berlin (IPFUB) in the 1970s. The outcrops are, respectively, distributed within a metric greyish mudstone layer, between the first and second sandy bioclastic limestones characterising the member. Although IPFUB sampled a locality also named ‘Porto das Barcas’, which provided some vertebrate microfossils (Hahn and Hahn 2001; Wiechmann 2003), no data nor coordinates could be found to help to locate it (T. Martin, pers. comm., 2021). Considering the extent of the Praia de Porto das Barcas (almost 2 km), and the extent of Jurassic exposures in the area, we cannot confirm we have sampled the same locality as the previous team. Therefore, we consider that the locality sampled by our team and referred as Porto das Barcas is not the same as the one sampled by IPFUB. Peralta VMA is located in the Praia Azul member, between the second and the third sandy bioclastic limestones, and so is younger than Zimbral and Porto das Barcas.

The exact age of the Guimarães beds had long been a matter of debate (Schudack 2000a), although they have consistently been considered as part of the Alcobaça Formation, which has been dated to the middle Kimmeridgian (Ribeiro et al. 1979; Mateus et al. 2017). Based on ammonites, charophytes, ostracods, pollens, and lithostratigraphic correlation, the age of the Guimarães beds is now restricted to the Kimmeridgian (Ribeiro et al. 1979; Leinfelder and Wilson 1989; Schudack et al. 1998; Schudack 2000a). Throughout the mining, around 20 m of the beds have been exposed (Helmdach 1971; Schudack 2000b). The outcrop consists of two coal seams of similar structure, with intercalation of lignitic marls occasionally rich in bivalve shells, separated by a single layer of limestone, around 5 m thick (Schudack 2000b).

Due to the mining conditions in Guimarães, the stratigraphic position of the specimens is uncertain, limiting the precise identification of the sedimentary environment where fossils were found. (Gloy 2000; Krebs 2000). Based on its similarity to other brown coal

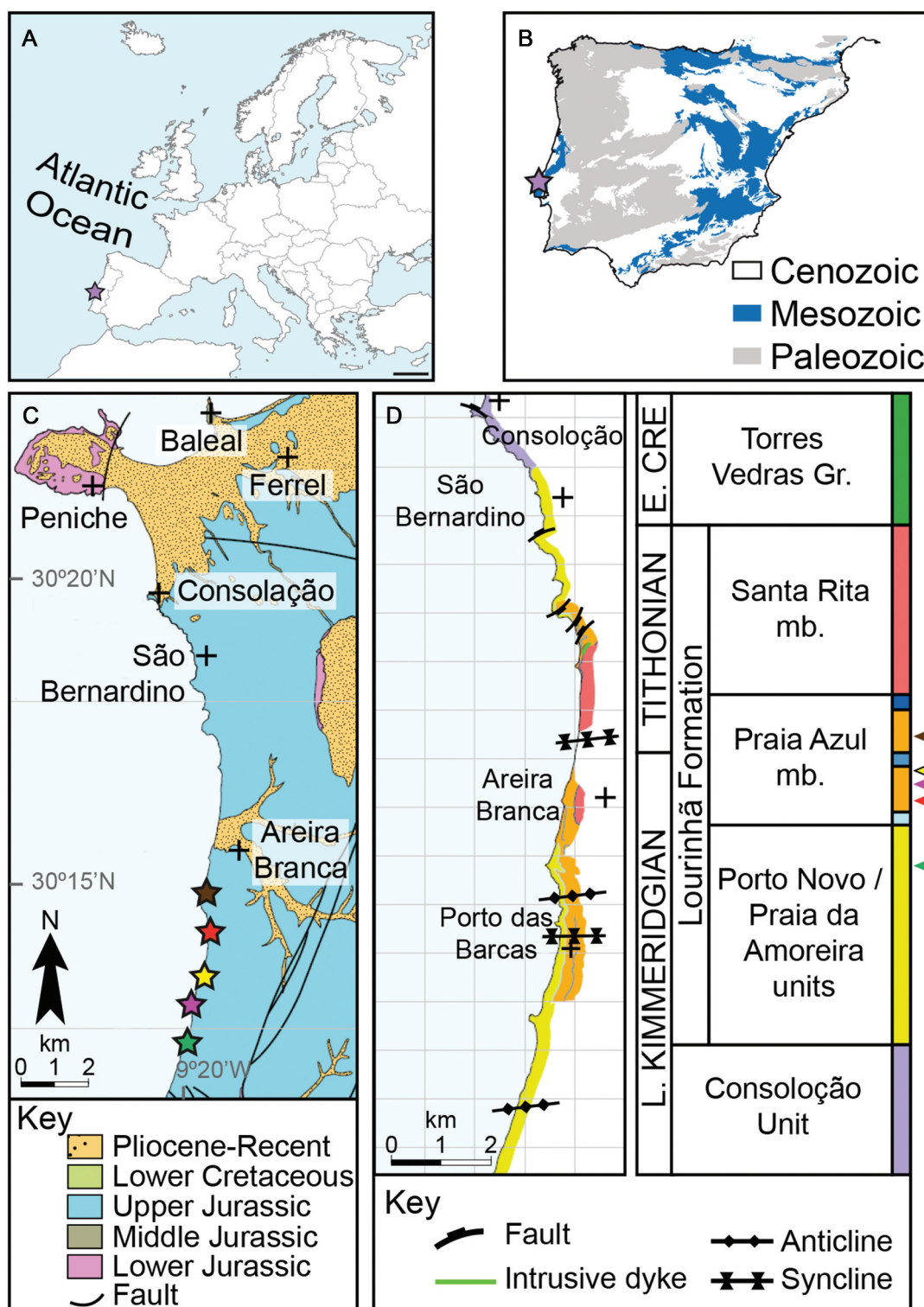


Figure 1. Geographical and geological context of the new Albanerpetontidae occurrences from the Lourinhã formation. **A**, Europe map modified from Erin Dill, scale represents 400 km. **B**, geological sketch of the Iberian Peninsula, showing the location of the study area (purple star). **C**, map of the onshore part of the Consolação subbasin south of Peniche (modified from Taylor et al. 2014). The green star indicates the location of the Valmitão VMA, the pink star indicates the location of Porto Dinheiro VMA, the yellow star indicates the location of Zimbral VMA, the red star indicates the location of Porto das Barcas VMA, the brown star indicates the location of Peralta VMA. **D**, north-south mapping of the main units in the area of study and their corresponding lithostratigraphic framework indicated by arrows (modified from Taylor et al. 2014, based on Mateus et al. 2017). Arrow colours correspond to star colours.

deposits and its geological setting, Guimarota has been regarded as a terrestrial to lagoonal environment similar to modern mangroves, with occasional freshwater influx and saltwater flooding (Gloy 2000; Martin 2000).

Material and methods

This study is based on a 700 kg sample of matrix collected from Valmitão, Zimbral, and Porto das Barcas (Lourinhã municipality, Portugal) during field campaigns between 2016 and 2019. One of us (CN) independently collected matrix on a regular basis over a period of several years, using bags of 5 kg each to an estimated total of between 100 and 150 kg, from two other localities: Porto Dinheiro and Peralta. The matrix was dried, then disaggregated in water with hydrogen peroxide (H₂O₂, final solution at 0.5%). The samples were screen-washed through a sieving table comprised of three levels of mesh (2 mm, 1 mm and 0.5 mm). The residues were then picked under stereomicroscopes. No significant differences in the degree of fracturing and preservation were observed between both samplings.

In total, around 20,000 microfossils from the three VMAs were recovered. Most of them consist of invertebrate remains, such as ostracods, gastropods, bivalve shells fragments, and charophyte thali. However, the vertebrate microfossils include ray-finned fish scales and teeth, chondrichthyan teeth, fragmentary material from lepidosaurs, amphibians and unidentified archosauriforms, crocodylomorph teeth and osteoderms, dinosaur and pterosaur teeth, tetrapod vertebral arches and long bone fragments, and eggshell fragments. Two hundred and eighty-five fossils are attributed to Albanerpetontidae, although cataloguing is still ongoing. The present study focuses on 34 frontals, none of which is complete, recovered from the 1 mm and 0.5 mm residue fractions (see Figure 2 for a composite reconstruction of the frontals based on ML2738). The specimens are housed in the Museu da Lourinhã (ML2738 to ML2749 and ML2751 to ML2772). Twenty-eight additional frontals (among 419 albanerpetontid fossil remains) from the private collection of one of us (CN) are now accessioned at the NOVA School of Science and Technology (FCT/UNL-CN00016 to FCT/UNL-CN00029, FCT/UNL-CN00100 to FCT/UNL-CN00108, and FCT/UNL-CN00398 to FCT/UNL-CN00402).

Fifty-eight additional specimens from the Alcobaça Fm. have been included. They all come from the excavations of the Guimarota beds by IPFUB. They were previously studied and presented (Wiechmann 2000), and resulted in an unpublished PhD thesis where they were informally assigned to a new species, '*Celtdens guimarotae*' (Wiechmann 2003). However, these specimens are here formally published for the first time. The specimen numbers attributed by IPFUB during the excavations were changed when the specimens were returned to the Museu Geológico de Lisbon, where they are now housed, following the agreements signed at the time of the excavations. Therefore, they are here published with their final accession numbers. Some of these specimens were already coated in gold (MG28502, MG28532, and MG28694) and MG28520 had fragments glued with Bostik Blu Tack™ by the previous authors. In some cases, the specimen numbers from MG may refer to several fragments, hence a total number of 58 frontals. Two specimens – MG28426, MG28427 – were assembled from multiple fragments of the same individual for imaging and measurements.

Specimens from the Lourinhã Fm. were photographed using a Canon Model RP reflex camera with a Canon 75–300 mm objective. The objective was coupled with a Nikon Microscope objective APOx10, mounted with an adapter ring. The specimens were laid on a vertical mounting setup with a MJKZZ stacking rail. The set up was remotely controlled with Stackrail 1.7, which allows automated capture for stacking (at least 70 steps for each specimen, 40 µm/slice). The RAW image files were converted to TIFF and homogenised using Digital Photo Professional 4. The stacking process was performed with Zerene Stacker 1.4. The resulting images were then fine-tuned, cleaned, and processed for final rendering. The specimens from the Alcobaça Fm. were photographed using a DinoLite AM7013MZT, using Dino software. The best-preserved specimens were measured with ImageJ (Rasband 2003) (see Table 1 and Figure 3).

Morphometric analysis

Measurements from 17 specimens (5 from the Lourinhã Fm., 12 from the Alcobaça Fm.) presented in Table 1 were used to perform linear morphometrics, with association of principal component analysis (PCA) and linear discriminant analysis (LDA). A first PCA was performed with all variables. However, this model

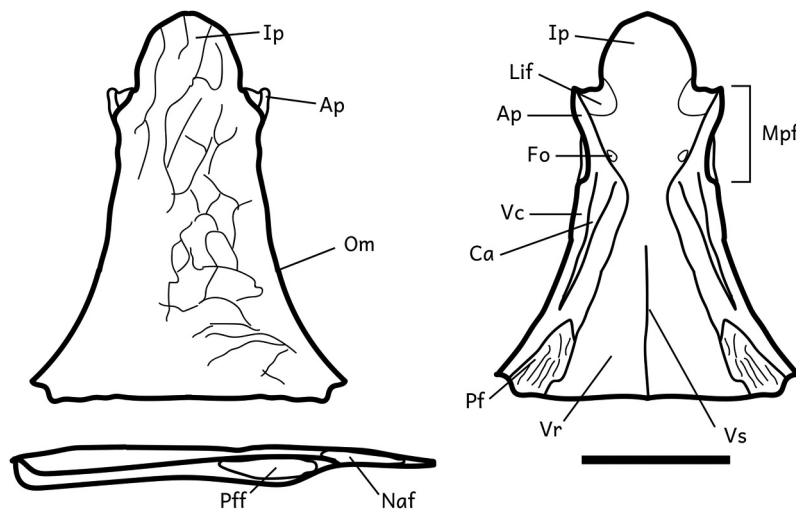


Figure 2. Main anatomical features of albanerpetontid frontal bones, based on reconstruction from specimen ML2738, in dorsal, ventral, and lateral views. **Ap**, anterolateral process; **Ca**, canal; **Fo**, foramen; **Ip**, internasal process; **Lif**, lateroventral internasal facet; **Mpf**, middle part of the frontal; **Naf**, nasal facet; **Om**, orbital margin; **Pf**, parietal facet; **Pff**, prefrontal facet; **Vc**, ventrolateral crest; **Vr**, ventral roof; **Vs**, ventromedian suture. Scale bar represents 1 mm.

Table 1. Measurements (in mm) of the best-preserved specimens. **FML**, frontal length at the midline; **FL**, frontal length at the midline; **FW**, frontal width across posterior edges; **FIW**, frontal inner width between ventrolateral crests, across posterior edges of the frontal roof; **INL**, internasal length at the midline; **INW**, internasal width at the base; **SW**, slot width between the posterior slots for the prefrontal; **IVCW**, interventrolateral crests width; **OML**, orbital margin length; **VCAW**, ventrolateral crest anterior width, behind prefrontal facets; **VCPW**, ventrolateral crest posterior width, before parietal facets; **CPE**, curvature at the posterior part of the edge (in degrees); **VCC**, ventrolateral crest curvature (in degrees).

Specimen	Locality	FML	FL	FW	FIW	INL	INW	SW	OML	IVCW	VCAW	VCPW	CPE	VCC
ML2738	Lourinhã	2.6	2.56	2.01	1.37	0.47	0.65	0.79	1.31	0.31	0.34	0.26	23	129.5
ML2739	Lourinhã			2.64	1.93			1.32	2.16	0.43	0.64	0.36	11.8	125.2
ML2741	Lourinhã					0.89	0.97	1.12		0.26	0.46			139.5
FCT/UNL-CN00016	Lourinhã					0.57	0.48	0.76		0.23	0.33			134.1
FCT/UNL-CN00018	Lourinhã					0.64	0.55	0.83		0.25	0.37			136
MG28426	Guimarota	5.85	6.35	4.35	1.52	0.76	1.42	2.16	3.52	0.31	0.89	0.84	18.6	130.6
MG28427	Guimarota		5.83	4.81	2.34	0.94	1.68	2.33	3.41	0.28	1.25	0.85	17	133.5
MG28473	Guimarota	3.99	4.07	2.31	1.24		0.71	1.24	2.02	0.31	0.6	0.41	11.7	142.1
MG28502	Guimarota	5.69	6.03	3.71	1.38	1.24	1.17	1.92	2.67		1.02	0.84	17.8	138.8
MG28520	Guimarota	4.76	4.9	3.48	1.37	1.19	1.68	1.34	2.61		0.8	0.66	14.9	
MG28521	Guimarota	5.76				0.85	1.5	1.94		0.48	0.76	0.61		149.4
MG28532	Guimarota	3.88				0.86	1.04	1.28		0.25	0.47	0.34	13.4	151
MG28543	Guimarota	3.27		2.02	1.25	0.65	0.74	1.23			0.53	0.26		
MG28694	Guimarota					1.05	1.27	1.89			0.91			
MG28733	Guimarota			1.6	1.1			1.05	1.3	0.27	0.44	0.26	12.7	135
MG28539	Guimarota			2.17	1.03			1.07	1.77	0.28	0.41	0.32	17.9	148.1
MG28692	Guimarota			2.46	1.52				1.65		0.56	0.33	21.9	

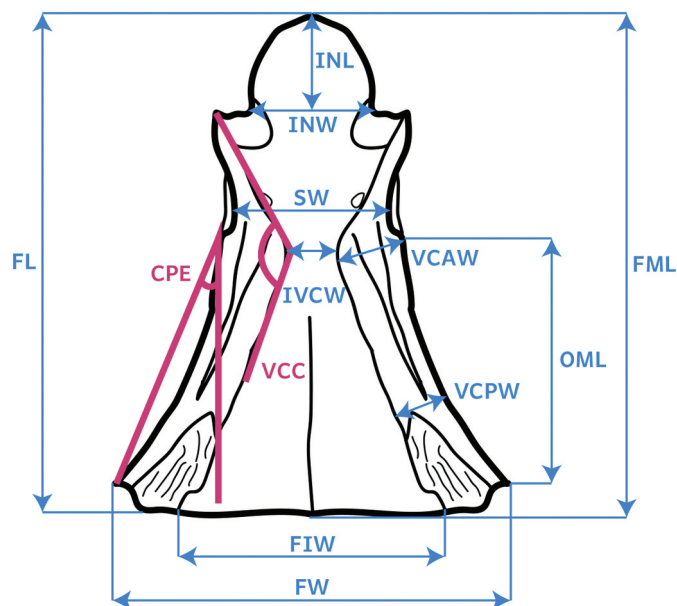


Figure 3. Measurements taken in the frontal bones represented in Table 1. Measurements in blue represent metric measurements; measurements in dark pink represent angle measurements. **CPE**, curvature at the posterior part of the edge (in degrees); **FIW**, frontal inner width between ventrolateral crests, across posterior edges of the frontal ventral roof; **FL**, total length of the frontal; **FML**, frontal length at the midline; **FW**, frontal width across posterior edges; **INL**, internasal length at the midline; **INW**, internasal width at the base; **IVCW**, inter-ventrolateral crests width; **OML**, orbital margin length; **SW**, slot width, between the posterior slots for the prefrontal; **VCAW**, ventrolateral crest anterior width, behind prefrontal facets; **VCC**, ventrolateral crest curvature (in degrees); **VCPW**, ventrolateral crest posterior width, before parietal facets.

appeared slightly underfitted, based on the broken stick model (Jackson 1993), as the second axis explains less variation than expected. This may represent a sampling bias: not only may there be too few specimens (17) relative to the number of variables (13), but may also be due to the fact that several specimens are highly fragmented. Indeed, only six specimens could provide measurements for at least 70% of the variables; and only seven variables could be measured in at least 70% of the specimens. Therefore, a second PCA was performed using only the seven variables in which

at least 70% of the specimens could be measured: INL, INW, SW, IVCW, VCAW, VCPW, and VCC (see Figure 3 for the measurement abbreviations and definitions). This model appears more robust, as the second axis eigenvalue is above the broken stick model, and is the one described and discussed below.

Both the LDA and PCA were run using Past 4.03 (Hammer et al. 2001). All specimens were used and grouped according to their provenance (Lourinhã or Guimarota beds). As the measures used different units and can have different scales, the analyses were performed using a correlation matrix. Missing values were treated with the iterative imputation option, as recommended by the authors (Hammer et al. 2001). The PC (principal components) scores from the second PCA were used to perform the LDA, to determine if the specimens could be distinguished in different groups. In order to determine the best optimal partitioning, K-means partition comparison was performed using R4.0.3, with the vegan 2.5–7 package (Oksanen et al. 2020). Firstly, K-means partitions comparison was performed to find the most optimal grouping of our specimens. Based on the Simple Structure Index (SSI), three groups appear to be the most optimal partitioning (SSI = 0.59), which was applied for the LDA. The highest SSI value is regarded as a good indicator of the best partition, as it multiplicatively combines several elements that influence the interpretability of a partitioning solution (Borcard et al. 2018; Oksanen et al. 2020). The comparison was set with number of groups of the cascade between 2 and 5, considering the sample size. However, as recommended by the author of the package, higher numbers of groups were explored. The confusion matrix of the LDA was corrected using Jackknifed resampling (leave-one-out cross-validation procedure; Hammer et al. 2001). Multivariate analysis of variance (MANOVA) was performed on the PCA scores using Pillai trace test to determine if there was a significant difference between the groups, coupled with a Pairwise post-hoc test using Bonferroni-corrected p values to determine which groups were significantly different to the others (Hammer et al. 2001).

The relationships between (1) the frontal inner width between ventrolateral crests, across posterior edges of the frontal ventral roof (FIW) and ventrolateral crest anterior width, behind prefrontal facets (VCAW); (2) the frontal length at the midline (FML) and the internasal length at the midline (INL); and (3) the slot width, between the posterior slots for the prefrontal (SW), and the frontal width across posterior edges (FW) were analysed with linear

regressions for sign of allometry, with, respectively, 11, 7, and 11 specimens due to the overall preservation in the sample. Measurements were log-transformed using the log function from PAST 4.03 before using them to run the linear model with R4.0.3, using the implemented R stats package and the package ggplot2 for visualisation and validating the model (Wickham et al. 2021). See Supplementary files 1 and 2 for R script and additional morphometric data used.

Phylogenetic analysis

Phylogenetic analyses were performed using TNT 1.5 (Goloboff and Catalano 2016). Both NEXUS files for the matrix were created with Mesquite 3.61 (Maddison and Maddison 2019) and exported as a .tnt file that was modified in a text editor to add the necessary settings and commands (see Supplementary files 3 and 4 for the TNT files).

The dataset used is based on the latest iteration of the Gardner (2002) dataset, published by Daza et al. (2020). Two additional characters were added based on new observations concerning the frontal bones of the different species (see Supplementary files 5 for the character list). The most recent iteration from Carrano et al. (2022) was not used as it was published late during the review process. The still uncertain position of Albanerpetontidae within Lissamphibia reflects the lack of a satisfactory outgroup. Previous studies have relied on a hypothetical – all 0 – outgroup, assuming 0 was the ancestral condition for each character without further phylogenetic evidence. We followed Matsumoto and Evans (2018) and Daza et al. (2020) in choosing *Anoualerpeton priscum* as our outgroup, because the genus *Anoualerpeton* has been consistently recovered as the basal-most Albanerpetontidae (Gardner et al. 2003; Venczel and Gardner 2005; Sweetman and Gardner 2013; Matsumoto and Evans 2018; Daza et al. 2020).

Most of the previous iterations of the dataset employed *Celtedens* only at a generic level, based mainly on the description of *Celtedens ibericus* McGowan & Evans 1995, because specimen LH 6020 from Las Hoyas is one of the few complete, articulated albanerpetontid fossils known. In the present analysis, as in the one of Carrano et al. (2022), *Celtedens* was incorporated as the two described species, *C. ibericus* and *Celtedens megacephalus* (Costa 1864).

The Portuguese specimens were coded as two terminal taxa, according to their geographic provenance (Guimarota or Lourinhã). All elements in both collections were scored for the purpose of the analyses, although this study focuses only on the frontals. Scoring for Lourinhã Fm. elements is based on the microfossils from our picking. Scoring for Alcobaça Fm. elements is based on previous work by Wiechmann (2003) and observations during the revision of the material. Scoring for other *Celtedens* taxa is based on the coding provided in the unpublished PhD thesis of Wiechmann (2003), complemented by descriptions and images available in the literature (McGowan 2002; Maddin et al. 2013). Two analyses were performed: one considering specimens from the Alcobaça Fm. and the Lourinhã Fm. as two different species; and the second considering only one species, with polymorphic characters when required. In the final dataset, 22 terminal taxa were selected for the first analysis, and 21 for the second coded for 38 unordered characters. For the same reason that the data set was not used, the new species described by Carrano et al. (2022) was not included. We used the species name following the emendation proposed by Marjanović and Laurin (2008). TNT requires the definition of a single outgroup, which would result in an artificial placement of *Anoualerpeton unicum* Gardner et al. 2003 as more related to all other Albanerpetontidae than to *Anoualerpeton priscum* contrary to

all previous analyses. To work around this problem, a taxonomic outgroup was defined for the genus *Anoualerpeton*, and all MPTs recovered in the different analysis were re-rooted to the taxonomic outgroup after the searches.

Two analyses were run in TNT, a first analysis using all equally weighted characters, and a second analysis using implied weights, to reduce the effect of homoplasy. Different K values were tested—with lower values causing more drastic downweighting of the homoplasy than higher values (Goloboff et al. 2008), but the results were the same for every K larger than 5. All results shown are using K = 12. The analyses were performed with a traditional search using 1000 replications of Wagner trees followed by tree bisection reconnection (TBR) saving 10 trees saved by replication; and an additional round of TBR was performed on the resulting most parsimonious trees (MPT) to further explore the tree space.

A strict consensus tree was generated from all the MPTs recovered by each analysis. Branch support was calculated using bootstrap standard resampling with 1000 replicates. Consistency and retention indexes were calculated for each MPT and each individual character using the script allstats.run by Peterson Lopes (Universidade do Sau Paulo, Brasil).

Systematic palaeontology

Amphibia Linnaeus 1758

Lissamphibia Haeckel, 1866

Albanerpetontidae Fox and Naylor, 1982

Genus *Celtedens* McGowan and Evans, 1995

aff. *Celtedens* sp. (Figures 4 & Figure 5)

Referred material

Sixty-two frontals from the Lourinhã Formation: ML2738 to ML2749; ML2751 to ML2772; FCT/UNL-CN00016 to FCT/UNL-CN00029; FCT/UNL-CN00100 to FCT/UNL-CN00108; and FCT/UNL-CN00398 to FCT/UNL-CN00402.

Fifty-eight frontals from the Alcobaça Formation: MG28426; MG28427; MG28444; MG28451 (two fragments); MG28459; MG28473; MG28488 (three fragments); MG28491; MG28500; MG28502; MG28516; MG28520; MG28521; MG28524; MG28527 (two fragments); MG28531; MG28532; MG28533; MG28536 (three fragments); MG28539; MG28541; MG28542; MG28543; MG28559; MG28562; MG28564 (four fragments); MG28569; MG28570; MG28571; MG28572; MG28639; MG28648; MG28667; MG28672; MG28673; MG28691; MG28692; MG28694; MG28707; MG28710; MG28713 (three fragments); MG28714; MG28717; MG28721; MG28732; MG28733.

Localities and age of the specimens

All 120 specimens studied come from the Upper Jurassic outcrops of the Lusitanian basin, in Portugal, distributed between 6 different localities: 24 specimens from late Kimmeridgian Valmitão VMA (Lourinhã Municipality, Portugal) in the Porto Novo/Praia da Amoreira Member of the Lourinhã Formation; 1 specimen from late Kimmeridgian Porto das Barcas VMA (Lourinhã Municipality, Portugal), in the Praia Azul member of the Lourinhã Formation; 6 specimens from late Kimmeridgian Porto Dinheiro VMA (Lourinhã Municipality, Portugal), in the Praia Azul member of the Lourinhã Formation; 25 specimens from late Kimmeridgian Zimbral VMA (Lourinhã Municipality, Portugal) in the Praia Azul Member of the Lourinhã Formation; 6 specimens from early Tithonian Peralta VMA (Lourinhã Municipality, Portugal) in the

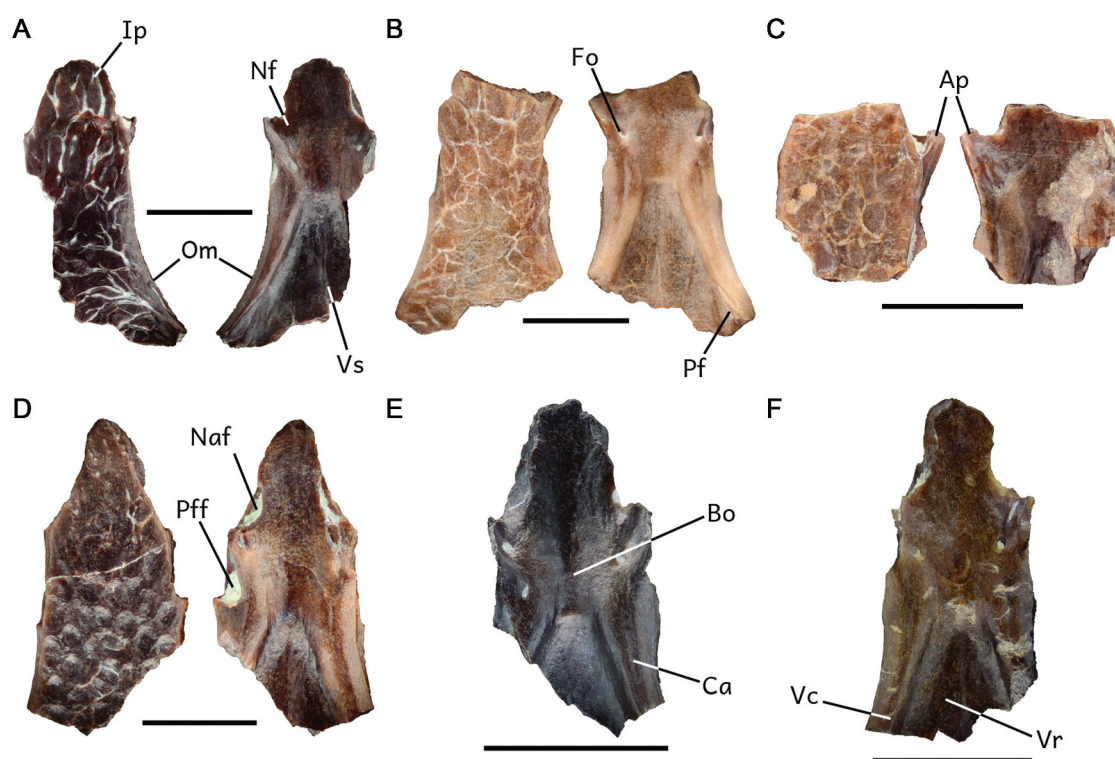


Figure 4. Normal-light photomicrographs of aff. *Celteledens* sp. frontal bones from the Lourinhã Formation in dorsal (left) and ventral (right) views. **A**, ML2738; **B**, ML2739; **C**, ML 2740; **D**, ML2741; **E**, FCT/UNL-CN00016; **F**, FCT/UNL-CN00018. Scale bars represent 1 mm.

Praia Azul Member of the Lourinhã Formation; and 58 specimens from the Guimarães beds (Leiria Municipality, Portugal) in the Kimmeridgian Alcoaça Formation.

Description

None of the Lourinhã Fm. specimens is complete, most of them preserve only a fragmented ventrolateral crest or the anterior part of the middle part of the frontal (see [Figure 2](#) for a composite reconstruction based on specimen ML2738, and for anatomical terminologies). Specimens from the Alcoaça Fm. display various states of preservation (see [Figure 5](#)), from ventrolateral crest fragments to almost complete specimens. Measurements and the abbreviations applying them throughout the descriptions that follow can be found in [Figure 3](#) and [Table 1](#). See supplementary file 6 for more details on the preservation of specimens.

The frontals exhibit bell-shaped ventral and dorsal outlines: after the anterolateral process, the edge expands posteriorly, parallel to the midline. However posteriorly, it is arched laterally. The FL/FW proportion (see [Figure 3](#)) is 1.27 in ML2738, the only specimen in which it could be measured in Lourinhã Fm, but varies from 1.21 to 1.76 in Alcoaça Fm. specimens (see [Figure 3](#) and [Table 1](#)). The orbital margin curvature at the posterior part of the edge (see [Figure 3](#)) is more marked in some specimens (ML2738, MG28692, MG28426) than others (ML2739, MG28473, MG28733), varying from 11.8° to 23° in the Lourinhã Fm. specimens, and from 11.7° to 21.9° in the Alcoaça Fm. specimens (see [Table 1](#)). The Lourinhã Fm. specimens display different degrees of dorsal surface ornamentation. Some, e.g., ML2738, exhibit a sculpture tiny grooves expressed as wiggly lines randomly arranged (now referred to as vermicular ornamentation, [Figure 4A](#)). In other specimens, e.g., ML2739, ML2740, or ML2742 (not figured), the ornamentation

may still present a vermicular pattern, but may also start to display polygonal pits typical of many albanerpetontids ([Figure 4B](#) and [C](#)). A third stage of ornamentation, as illustrated by ML2741, FCT/UNL-CN00016, and FCT/UNL-CN00018, is characterised by deep, polygonal pits with irregular honeycomb ornamentation ([Figure 4D](#)). None of the Alcoaça Fm. specimens display vermicular dorsal ornamentation. When preserved and not eroded, their dorsal surfaces exhibit one of the two other degrees of ornamentation, with polygonal concave pits of various shapes (irregular polygonal to honeycomb).

The internasal process is spatulate to flabellate, with a bulbous broad shape more or less pronounced from one specimen to another, in ventral and dorsal views ([Figure 4A](#), [D](#), [E](#), and [F](#); and [Figure 5B](#), [D](#), [F](#), [G](#), and [O](#)), with a INW/INL proportion of 0.84 to 1.38 in Lourinhã specimens, and of 0.94 to 1.87 in the Alcoaça Fm. specimens (see [Figure 3](#) and [Table 1](#)). Each edge bears a deep, longitudinal anterior slot for the nasal facet ([Figure 4A](#) and [D](#)).

When preserved, the anterolateral processes are distinct from the middle part of the frontal and can be seen in dorsal view ([Figures 4A](#), [C](#), and [E](#); and [Figures 5C](#), [D](#), [F](#), [M](#), and [O](#)). The process displays an acuminate apex and extends anterolaterally, and yields a deep, lateral slot-facet expanding posteriorly towards the orbital margin comprising the prefrontal facet ([Figures 2](#) and [Figure 4D](#)). When preserved, the process is short in most specimens, although its expansion varies from one specimen to another, and it can be distinct from the middle part of the frontal, e.g., ML2740 ([Figure 4C](#)), MG28444, MG28491, and MG28639 (not figured).

The ventral surface of the nasal facet does not broaden laterally, and the facet cannot be seen in dorsal view, except in ML2741, although this could represent an artefact of preservation. The ventral surface of the internasal process and the middle part of the frontal is flat to weakly concave in the



Figure 5. Normal-light photomicrographs of aff. *Cetedens* sp. frontal bones from the Alcobaça Formation in dorsal (left) and ventral view (right). **A**, MG28426; **B**, MG28427; **C**, MG28473; **D**, MG28502; **E**, MG28520; **F**, MG28521; **G**, MG28532; **H**, MG28539; **I**, MG28541; **J**, MG28543; **K**, MG28562; **L**, MG28570; **M**, MG28572; **N**, MG28692; **O**, MG28694; **P**, MG28733. Scale bars represent 1 mm.

longitudinal axis. Medial to the anterior-most part of the anterolateral processes, the ventral surface of the internasal process bears a faint, triangular facet (Figures 4A and C), which would articulate with the nasal and/or the lacrimal. Ventrally, the anterolateral process expands posteriorly and medially into a thin ridge following the edge where it meets the ventrolateral crest. A foramen, connected to the canals of the ventrolateral crests, is present at the anterior-most part of the ventrolateral crests, where the anterolateral process ridges and the lateroventral internasal facets end (Figure 4A, B, and E; and Figure 5F, K, and P). The slot width between the posterior slots for the prefrontal is smaller than the frontal width across the posterior edges (see Figure 3), with a SW/FW proportion between 0.39 and 0.5 in the Lourinhã Fm. specimens, and between 0.39 and 0.66 in the Alcobaça Fm. specimens (see Table 1).

The ventrolateral crests are broadest anteriorly, with a VCAW/VCPW proportion from 1.31 to 1.78 in Lourinhã specimens, and from 1.06 to 2.04 in the Alcobaça Fm. specimens (see Table 1). However, they do not meet medially in any specimen in which both sides are preserved (Figures 4A, B, D, E, and F; and Figure 5A, B, F, G, H, I, K, L, M, P). The ventrolateral crests are convex ventrally and are ridge-like in transverse profile. The more lateral part along the orbital margin is bevelled and faces ventrolaterally. The ventrolateral crests exhibit a shallow groove, forming a canal that extends anteroposteriorly from the prefrontal facet to the parietal facet (Figures 4A, B, and D), or fades into a rugose surface at the middle of the crest in ML2738 and ML2741. In the Alcobaça Fm. specimens, this groove can be eroded or not visible, but extends as far as the parietal facet in MG28473 (Figure 5C).

When the frontal ventral roof is preserved, a weak ventromedian suture extends anteriorly towards the middle part of the frontals (Figures 4A, B, D, and F).

Remarks

Frontal bones from the Lourinhã Fm. and the Alcobaça Fm. are generally similar. They share: (1) the same general bell-shaped outline; (2) a flabellate, bulbous-shaped internasal process; (3) small acute anterolateral processes; (4) ventrolateral crests convex ventrally and ridge-like in transverse profile, with the orbital margin bevelled and facing ventrolaterally; and (5) a weak ventromedian suture extending anteriorly towards the middle part of the frontals. Differences can be noted between the Portuguese specimens, especially in the curvature of the orbital margin, the extension of the ventrolateral crest canal, and the dorsal ornamentation. However, these differences occur not only between the Lourinhã Fm. and the Alcobaça Fm. specimens, but also among specimens from same geographic origin. These differences may result from ontogenetic or environmental factors leading to ecophenotypic and intraspecific variations (McGowan 1998; Wiechmann 2003). See intraspecific and ontogenetic variation in the discussion that follows for more details on this aspect. Thus, based on their frontal bones, all Portuguese albanerpetontid specimens are conservatively attributed to aff. *Celtedens* sp. However, more research on other skeletal elements is required to determine with certainty if specimens from the Lourinhã Fm. and the Alcobaça Fm. are congeneric and conspecific.

Celtedens sp. differs from *Albanerpeton sensu lato* (*Albanerpeton* s.l.), *Shirerpeton*, *Wesserpeton*, the Uña specimen, and *Yaksha* by having a bell-shaped outline, a bulbous flabellate internasal process (Sweetman and Gardner 2013; Matsumoto and Evans 2018; Daza et al. 2020). It differs from *Shirerpeton*, *Yaksha*, and the specimen from Uña by lacking an anterior contact between the ventrolateral crests, from *Albanerpeton* s.l. and *Shirerpeton* by having short anterolateral processes rather than long (Matsumoto and Evans 2018), from *Albanerpeton* s.l. and *Yaksha* by being rather more elongated than wide (Daza et al. 2020). It resembles *Wesserpeton* in displaying short anterolateral processes (Sweetman and Gardner 2013). The bell-shaped outline, the flat ventral surface of the internasal process and short acute anterolateral process constitute features found in *Anoualerpeton*. However, aff. *Celtedens* sp. contrasts with this genus by having a flabellate internasal process with bulbous and broad shape (Gardner et al. 2003).

Aff. *Celtedens* sp. shares the morphology of the frontal recognised in *Celtedens*, especially the general outline (bell-shaped to hourglass in *Celtedens*) and the flabellate, bulbous-shaped internasal process. The orbital margin appears laterally curved in aff. *Celtedens* sp. of Portugal, as it is observed in *C. megacephalus* (Estes 1981; McGowan 1998, 2002). Although the orbital margin curvature is posteriorly less pronounced in some specimens (ML2739, MG28473, MG28733) or appears less pronounced as an artefact of preservation (ML2741, FCT/UNL-CN00016, FCT/UNL-CN00018, MG28521, MG28543, MG28594), it does not exhibit the hourglass shape observed in *C. ibericus* (McGowan and Evans 1995; McGowan 2002) either. Also, based on what could be observed in published figures of *C. megacephalus* and *C. ibericus*, aff. *Celtedens* sp. shares with *C. megacephalus* a narrower anterior inter-lacrimal width to posterior parietal margin width (Figure 3) than *C. ibericus*, with a proportion ranging between 0.39 and 0.66 in both localities

(Table 1). Unfortunately, the anterior part of *C. megacephalus* frontal from Pietrarroia remains unknown (McGowan 2002), and therefore cannot be compared with Spanish specimens from Uña attributed to that species (Wiechmann 2003) or with Portuguese specimens, although ML2738 might be similar. Moreover, Pietrarroia is dated from the early Aptian of Benevento Province in Italy, and the Uña referred but unconfirmed specimen is from the late Barremian. Thus, based on the anatomy of their frontal bones and their geographical and time separation, it can be concluded that even though they share affinities, Portuguese specimens of aff. *Celtedens* sp. are not conspecific with either *C. megacephalus* or *C. ibericus*.

Results

Morphometric analysis

Linear morphometric analysis

The three first axes of the PCA account for 95.6% of the variation. For the PC1-PC2 graph in scaling 1 (Figure 6; A), the larger specimens are grouped together in positive values in PC1 and PC2, except MG28520 that has a negative value in PC2; while the others are grouped together in the negative values in PC1 and spread in positive and negative values in PC2. However, ML2739 presents a higher value in PC2 than the others. For the PC3-PC2 graph in scaling 1, most of the specimens are grouped together towards the centre of the graph, with a negative value for PC3, to a lesser extent for ML2739 and the duo MG28539-MG28532. However, MG28521 presents high positive values in PC3 and is associated with higher values of IVCW and VCC. All PCA scores are presented in Supplementary file 2.

For the PC1-PC2 graph in scaling 2 (Figure 6; B), all variables are positively correlated to PC1. Meanwhile, VCPW, VCAW, SW, and IVCW are positively correlated to PC2; and INW, INL, and VCC are negatively correlated to PC2. For the PC3-PC2 graph in scaling 2, SW, VCAW, and VCPW are negatively correlated to PC3. INL is almost not correlated to PC3. INW is weakly positively correlated to PC3, while IVCW and VCC are both highly positively correlated to PC3. All PCA loadings (coefficient and correlation) are presented in Supplementary file 2. Additional description of the results from the PCA are presented in Supplementary file 6.

All the variation is explained by the two main axis of the LDA (see Figure 7). Group 1 is composed of only five specimens from the Alcobaça Fm.; group 2 is composed of only four specimens, including one from the Lourinhã Fm.; group 3 is composed of eight specimens, including four from the Lourinhã Fm. The confusion matrix corrected by Jackknifed resampling correctly classified 88.24% of the specimens. The MANOVA performed on the scores from the PCA confirms there is a significant difference between the groups (Pillai trace test; $F = 5.025$; $df_1 = 14$ and $df_2 = 18$; $p\text{-value} = 0,0009048$), and the post-hoc test that group 1 and group 3 are significantly different ($p\text{-value} = 0,021737$), but group 2 is not significantly different with either group 1 or group 3.

Linear regression

The first linear regression is set to compare the relationship between ventrolateral crest anterior width, behind the prefrontal facets, and the frontal inner width between the ventrolateral crests (Figure 8; A). Considering those parts of the bone are among the most commonly

preserved, 11 specimens could be used. The slope equation (1) is higher than 1. The adjusted R^2 is 0.3617, the p-value lower than 0.05 supports the conclusion that the results are significant, and the residuals behave normally and respect the homoscedasticity (homogeneity

of the variance between all values of the residuals; see Supplementary file 1).

$$\text{Log}_{VCAW} = 1.10968 \times \text{Log}_{FIW} - 0.36888 \quad (1)$$

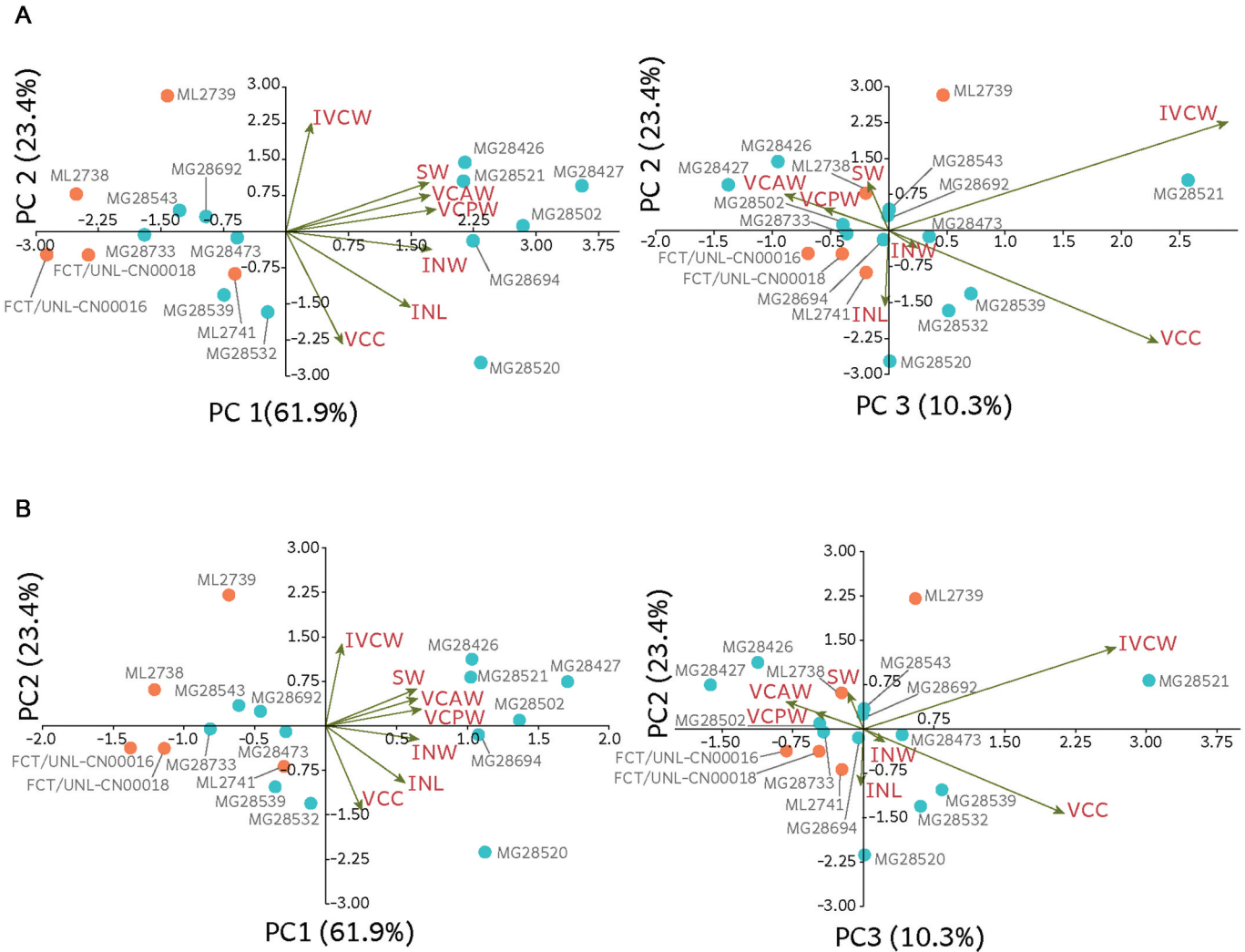


Figure 6. Principal component analysis based on 7 variables in scaling 1 (A) and scaling 2 (B). Orange dots represent specimens from the Lourinhã Formation, blue dots represent specimens from the Alcobaça Formation.

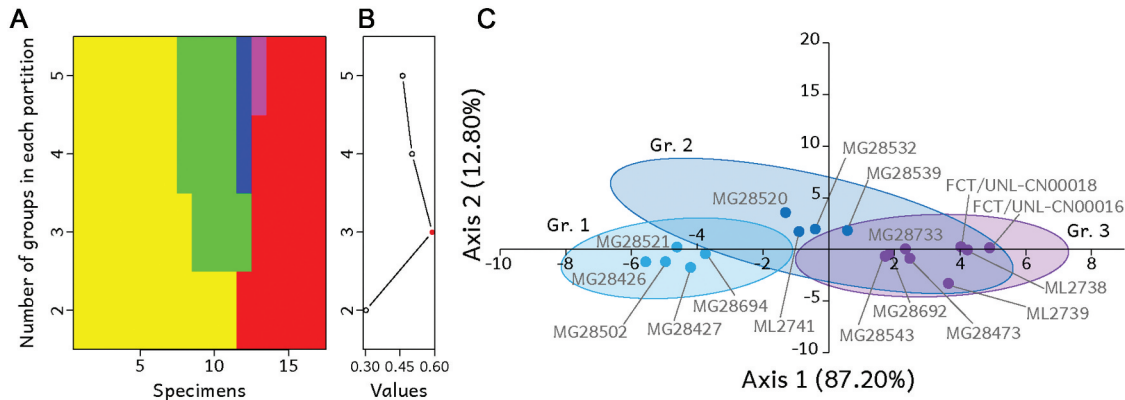


Figure 7. A, K-means partitions comparison; each colour represents a different group to which the specimens (x-axis) are attributed. B, Simple Structure Index criterion corresponding to each partition (best SSI = 0.59). C, Linear discriminant analysis (confusion matrix with Jackknifed resampling = 88.24%).

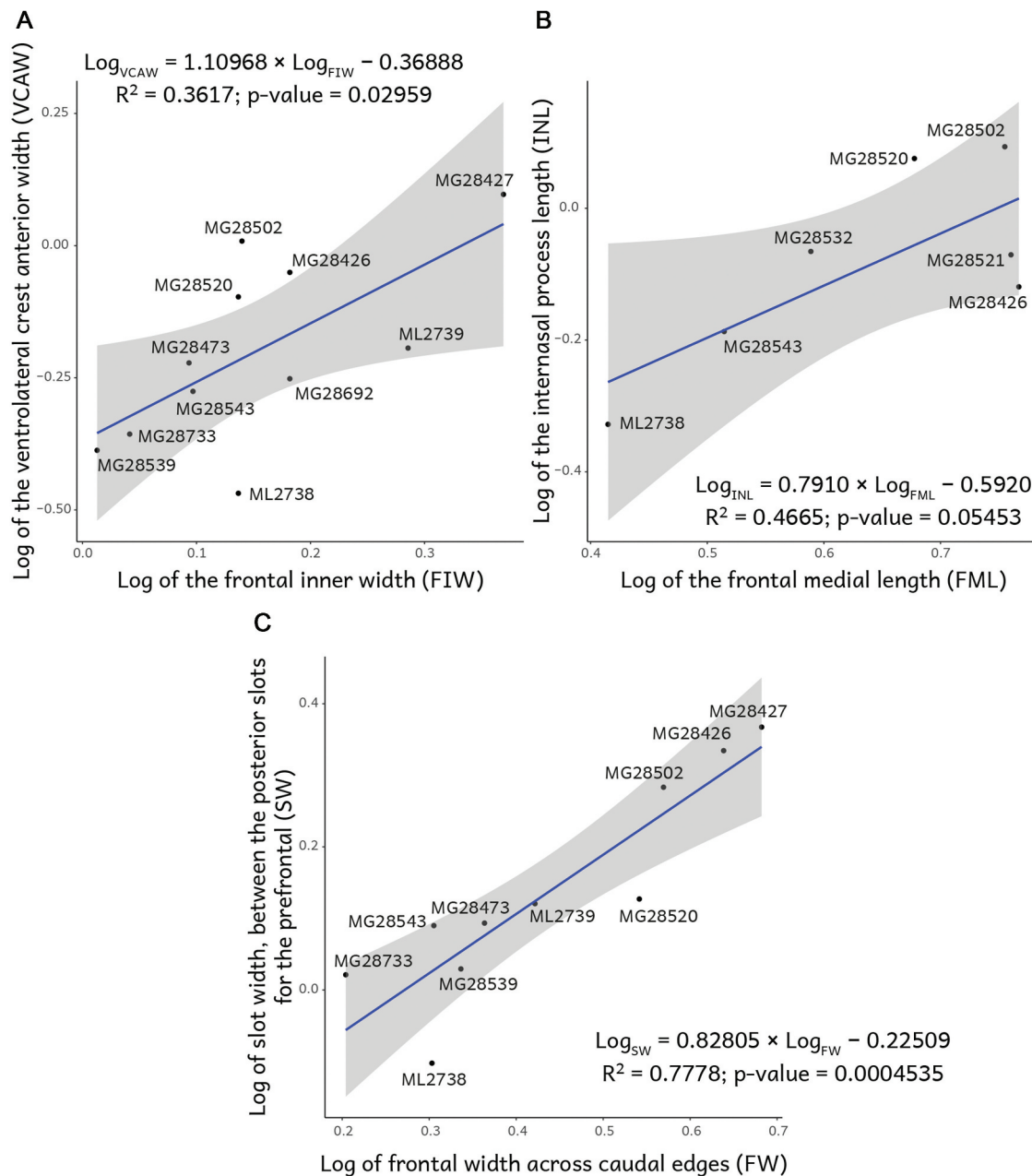


Figure 8. Linear regression to test the allometry in the ventrolateral crests (A), the internal nasal process (B), and slot width, between the posterior slots for the prefrontal (C). The blue line represents the model, and the grey area the 95% confidence interval.

The second linear regression is set to compare the relationship between the internal nasal process length and the frontal medial length (Figure 8; B). Only 7 specimens could be used. The slope equation (2) is lower than 1. The adjusted R^2 is 0.4665, but the p-value is 0.05453, and therefore the results are non-significant. The normality and the homoscedasticity of the residuals could not be certified, but they seem to respect those hypotheses (see Supplementary file 1).

$$\text{Log}_{\text{INL}} = 0.7910 \times \text{Log}_{\text{FML}} - 0.5920 \quad (2)$$

The third linear regression is set to compare the relationship between the slot width, between the posterior slots for the prefrontals, and the frontal width across posterior edges (Figure 8; C). For this one, 11 specimens could be used. The slope equation (3) is lower than 1. The adjusted R^2 is 0.7778, and the p-value lower than

0.05 supports the conclusion that the results are significant. The residuals behave normally and respect the homoscedasticity (see Supplementary file 1).

$$\text{Log}_{\text{SW}} = 0.82805 \times \text{Log}_{\text{FW}} - 0.22509 \quad (3)$$

Phylogenetic analysis

In the first analysis considering two different Portuguese species, 10 MPTs were recovered during the analysis, with a fit of 2.07857 and 73 steps (see Figure 9). The consistency index (CI) is 0.603 and the retention index (RI) is 0.724. The inclusion of *Celtesdens* specimens collapsed the genus and produced a basal polytomy with a clade comprised of all other albanerpetontids. This latter clade includes a basal trichotomy, between *Wesserpeton evansae* Sweetman and

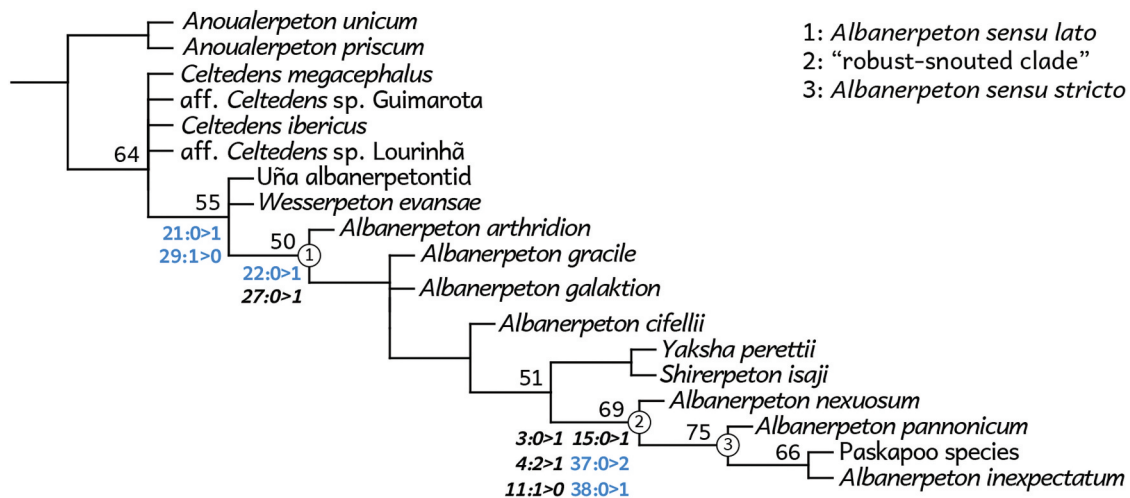


Figure 9. Consensus tree of the 10 MPTs recovered under implied weights. Fit = 2.07857; length = 73 steps; CI = 0.603, RI = 0.724. black numbers are bootstrap values to the corresponding nodes. bold number are synapomorphies (italic not related to the frontal bones, blue related to the frontal bones). **Node 1**, *Albanerpeton* s.l.; **Node 2**, ‘robust-snouted clade’; **Node 3**, *Albanerpeton* s.s.

Gardner 2013, the Uña specimen – which has been described as *Wesserpeton* sp. (Sweetman and Gardner 2013) – and another monophyletic clade comprised of all other albanerpetontids, previously described as *Albanerpeton* s.l. (Daza et al. 2020). As already pointed out in most recent studies, the genus *Albanerpeton* is recovered as a paraphyletic taxon (Matsumoto and Evans 2018; Daza et al. 2020), with the two most recently described albanerpetontid species, *Yaksha perettii* Daza et al. 2020 and *Shirerpeton isajii*, nesting within *Albanerpeton* s.l., and forming a clade sister to the informally named ‘robust-snouted clade’ (Gardner and Böhme 2008). A trichotomy is also recovered between *Albanerpeton galaktion*, *Albanerpeton gracile* Gardner 2000b, and the clade comprised of more nested Albanerpetontidae. In this topology, the Cenozoic species still form the most derived clade, referred to *Albanerpeton* s. s. Note the general low support of these clades, with few values over 50, and only the clade *Albanerpeton* s.s. and clades within show a bootstrap value over 65.

However, the results from the linear morphometric analyses were inconclusive concerning the question of whether specimens from the Alcoaça Fm. and the Lourinhã Fm. form two distinct species, or if they are conspecific. Therefore, a second analysis was

performed, using only one species with two polymorphic characters (char. 6 and char. 26) to represent all its variability. Only one MPT was recovered in this analysis (Figure 10), with a fit 1.99066, and 72 steps (one step shorter than the first tree). The CI is 0.611 and the RI is 0.714, which are also similar to the first analysis.

The global topology is similar to the previous analysis, with similarly low branch support, but this analysis resolves the basal polytomy, recovering *Celtenham* as a monophyletic genus sister to all other non-*Anoualerpeton* Albanerpetontidae. *W. evansae* is here recovered basal to the Uña specimen. Within *Albanerpeton* s.l., the only difference with the previous analysis is the resolution of the trichotomy within this clade, with *Albanerpeton arthridion* Fox and Naylor 1982, *A. galaktion* and *A. gracile* being recovered as successive sister clades of all other *Albanerpeton* s.l. In view of the taxonomic uncertainty regarding the Portuguese specimens, this analysis will be used for discussion.

Based on the character set used herein, *Albanerpeton* s.l. is characterised by two unambiguous synapomorphies: ‘moderate’ ratio of midline length of fused frontals versus width across posterior edge of bone (char. 22: 1); and anterior end of orbital margin in line with or behind the anteroposterior midpoint of frontals (char.

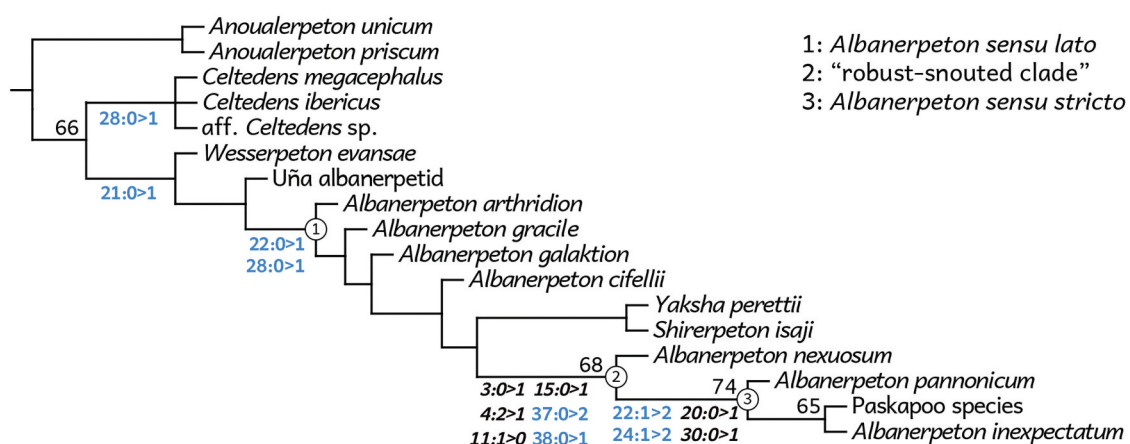


Figure 10. Consensus tree of the 1 MPT recovered under implied weights. Fit = 1.99066; length = 72 steps; CI = 0.611, RI = 0.714. black numbers are bootstrap values to the corresponding nodes. bold number are synapomorphies (italic not related to the frontal bones, blue related to the frontal bones). **Node 1**, *Albanerpeton* s.l.; **Node 2**, ‘robust-snouted clade’; **Node 3**, *Albanerpeton* s.s.

Table 2. Main indexes calculated for the MPT, and each character considered for the frontal bones.

		Character states	Minimum possible changes	Total changes	Consistency index CI	Retention Index RI	Times recovered as synapomorphy
MPT	-	82	44	72	0,611	0,714	49
Ch. 21	Dorsal or ventral outline of fused frontals	2	1	1	1	1	1
Ch. 22	Ratio of midline length of fused frontals versus width across posterior edge of bone	3	2	2 ¹	1	1	2
Ch. 23	Proportions of internasal process on fused frontals	2	1	5	0,333	0,6	2
Ch. 24	Form of ventrolateral crest on large, fused frontals	3	2	5	0,4	0,25	5
Ch. 28	Position in frontals of anterior end of orbital margin relative to anteroposterior midpoint of frontals	2	1	1	1	1	1
Ch. 29	Dorsal or ventral outline of internasal process on frontals	2	1	1	1	1	1
Ch. 31	Flattened ventromedian keel extending along posterior two thirds of fused frontals	2	1	6	0,25	0,4	4
Ch. 37	Frontal-lacrimal contact	3	2	3	0,667	0,667	2
Ch. 38	Edge of ventrolateral crests, position along the orbital margin	2	1	2	0,5	0,5	2

28: 1). The ‘robust-snouted clade’ is characterised by six unambiguous synapomorphies: inter-premaxillary contact fused medially (char. 3: 1), premaxillary pars dorsalis minimally overlaps and strongly sutured with anterior end of nasal (char. 4: 1), outline of suprapalatal pit oval (char. 11: 0), short premaxillary lateral process on maxilla relative to height of process at base (char. 15: 1), medial emargination of the prefrontal facet, making a notch visible dorsally and ventrally (the lacrimal sits lateral to the frontal) (char. 37: 2), and edge of ventrolateral crests medial to the orbital margin creating a ventral step, or parapet (char. 38: 1). *Albanerpeton* s.s. is characterised by four unambiguous synapomorphies: anterior end of maxillary tooth row approximately in line with the point of maximum indentation along leading edge of nasal process (char. 20: 1); ‘short’ (equal to or less than about 1.0) ratio of midline length of fused frontals versus width across posterior edge of bone, between lateral edges of ventrolateral crests, in large specimens (char. 22: 2); wide and triangular ventrolateral crest on large, fused frontals in transverse view, with ventral face deeply concave (char. 24: 2); and suprapalatal pit divided in about one–third or more of specimens (char. 30: 1).

Celtedens is recovered as a monophyletic group characterised by a single unambiguous synapomorphy: bulbous dorsal or ventral outline of internasal process on frontals (char. 29: 1). *C. megacephalus* is coded for 9 characters, and all are shared with both *C. ibericus* and aff. *Celtedens* sp. The only differences relate to an ambiguity in *C. megacephalus* (coded ‘?’). Of these nine characters, only one does not relate to the frontal bones (labial or lingual of occlusal margin of maxilla and dentary essentially straight, char. 18: 0). Likewise, aff. *Celtedens* sp. and *C. ibericus* share 23 characters in total, but none of them are exclusive as they are either ambiguous or also shared in *C. megacephalus*. Aff. *Celtedens* sp. from Portugal differs from *C. ibericus* in two characters: low ratio (less than about 1.55) of height of premaxillary pars dorsalis versus width across suprapalatal pit (char. 2: 1), and presence of flattened ventromedian keel extending along posterior two thirds of fused frontals (char. 30: 1). However, both are also ambiguous in *C. megacephalus*. Eight more characters were recovered in aff. *Celtedens* sp. but are ambiguous in both *C. ibericus* and *C. megacephalus*. Likewise, three characters were recovered in *C. ibericus* but are ambiguous in both *C. megacephalus* and aff. *Celtedens* sp. from Portugal. Finally, two characters were ambiguous in all *Celtedens* species (char. 7: distribution of labial ornament on large premaxillae; char. 27: path followed by canal through pars palatinum in premaxilla, between dorsal and ventral openings of palatal foramen).

Due to the high number of character state transformations observed in the characters relating to the fused frontal bones, we calculated individual consistency, and retention indices for each

character (Table 2). Five characters (21, 22, 28, 29, and 37) show consistency indexes over the global consistency index of the matrix, whereas 4 of them (23, 24, 32 and 38) show a lower consistency index, implying these characters have more homoplasy than the average for the most parsimonious tree. In addition, these four characters, together with character 37, show a lower retention index than the MPT, implying they have less homology than the average.

Discussion

Intraspecific and ontogenetic variation

Morphometrics

As expected, PC1 suggests a strong component linked to size, as shown by the positive correlation of all variables and the dispersion pattern of the specimens, with smaller ones towards the left and larger ones towards the right (Figure 6). However, the variation explained by PC2 and PC3 does not seem to have a specific dispersion pattern, preventing any clear biological variable being drawn from them. Only MG28521 (Figure 5F) appears distinct from the others, although this could be due to a preservational bias. The LDA succeeded in correctly classifying all specimens in a most-optimal grouping of 3. Group 1 and Group 3 are significantly different, but not from Group 2, which could indicate a continuity in the sample, with specimens from different ontogenetic stages. Indeed, all large specimens from the Alcobaça Fm. that were already near each other in the PCA are present in Group 1, except for MG28520 (Figure 5E), classified in Group 2. The same can be said with Group 3 which contains, among others, the smallest specimens. The high confidence interval observed for Group 2 could be due to the low number of specimens classified in it.

Furthermore, the pattern of the SSI criterion for inferring the most optimal group partitioning suggests a continuity in the sample. Partitions of 3 to 9 groups tend to have SSI values oscillating irregularly between 0.46 and 0.87 (see Figure 11). However, the values of SSI increase drastically with between 10 and 15 different groups, before forming a plateau between 1.35 and 1.48. Another increase occurs with 16 groups (SSI = 2.80), which is the maximum possible considering the sample size. That would indicate specimens are more optimally partitioned when they are alone than when grouped with other specimens, which is against the aim of grouping specimens together to find a pattern. This is interpreted as a sign of the continuity of the sample, rather than a true categorisation.

¹The number of character changes can be up to 4, due to the ambiguous codification of this character for *Yaksha* and *Shirepeton* (either 0 or 1, but never 2). Nevertheless, the optimization criteria used by TNT always prefers the shortest option, thus reducing the score of this character to 2.

Anatomical features

Intraspecific anatomical variations in the frontals of *Albanerpetontidae* have previously been reported and some attributed to ontogeny. One of the most common is variation in dorsal ornamentation: while the adults present the characteristic deep, polygonal ornamentation, with irregular to honeycomb pits; the juveniles present a shallow polygonal ornamentation (Gardner 1999a, 1999b, 2000a, 2000b; Gardner et al. 2003; Wiechmann 2003). This variation can be seen in the Portuguese specimens, but here a third stage is also observed. Some specimens (e. g. ML2738, Figure 4A) exhibit a vermicular ornamentation where the characteristic pattern is absent. The ventrolateral crest is also wider and extends posteriorly after the parietal margin in specimens representing adults. This is well illustrated by the difference between ML2738, where the unbroken ventrolateral crests end right before the parietal margin, while in MG28502 (Figure 5D) they appear relatively larger and extend beyond it. It has also been proposed that the ventromedian suture could be a sign of ontogeny, as it is less marked in adults (Gardner 1999b; Gardner et al. 2003; Wiechmann 2003; Venczel and Gardner 2005). The Portuguese specimens seem to present the same pattern, although for those from the Alcobaça Fm. it is difficult to assess whether this represents a taphonomic artefact or relate to the gold coating. The proportion between ventrolateral crest anterior width, behind the prefrontal facets, and the frontal inner width between the ventrolateral crests (VCAW/FIW) may also relate to ontogeny (Gardner 1999b, 2000b; Gardner et al. 2003; Wiechmann 2003; Venczel and Gardner 2005). In Portuguese specimens preserving both measurements, a significant linear response can be observed between their log-transformed values, even though the low adjusted R^2 could explain the large 95% confidence interval. Larger specimens tend to have wider ventrolateral crests, which is confirmed by the positive allometry, suggesting that the ventrolateral crest anterior width grows relatively faster than the frontal inner width in adult specimens from Portugal. However, our observations of the Alcobaça Fm. specimens contradict those of a previous study concerning these specimens (Wiechmann 2003), both in the range of variation of the VCAW/FIW proportion and its interpretation. Indeed, an interval of between 0.3 and 0.37 was reported, with a decline observed in larger individuals (Wiechmann 2003), while among the 11 specimens studied here, the VCAW/FIW proportion ranges from 0.25 to 0.74 (0.37 to 0.73 among the 9 specimens from the Alcobaça Fm), with an increase in larger specimens. It is still uncertain why such a dramatic contradiction is reported between the measurements of the same specimens, as they were taken following the same methodology. The VCAW/FIW proportion has also been used as diagnostic for *A. inexpectatum*, where it can reach higher values than 0.6, while fluctuating between 0.25 and 0.40 in other published species (Gardner 1999b; Wiechmann 2003). However, data from the Portuguese specimens suggests this character needs to be reviewed in other species to clarify its taxonomic relevance. It was also proposed that the internasal process is relatively shorter in adults (Gardner 1999b; Gardner et al. 2003; Sweetman and Gardner 2013). Portuguese specimens present a linear response between the log-transformed values of the internasal process length and the frontal medial length. The slope suggests a negative allometry, confirming that the internasal process is relatively shorter in adults. However, the results are not significant and residual behaviours could not be properly interpreted. Both could be due to the low number of specimens (7) that preserved both measurements. Therefore, we cannot draw definitive conclusions on this anatomical feature and more and better-preserved specimens are required. Additionally, the relation of the slot width, between the posterior slots for the prefrontal (SW), to the frontal width across posterior edges (FW) was also analysed, in this study. Indeed, it has not been proposed to be subject to intraspecific variation, but it is part of the diagnosis of *C. ibericus*, whose SW/FW proportion is equal (or near to) 1, and *C. megacephalus*, whose SW/FW

proportion is characterised as lower than 0.5 (McGowan and Evans 1995; McGowan 1998). In Portuguese specimens, the proportion ranges from 0.39 to 0.66. The negative slope from the linear response suggests a negative allometry, meaning that frontal width across posterior edges is relatively smaller than the slot width in adults.

Above mentioned intraspecific variations that can be linked to ontogeny suggest that the Lourinhã Fm. and the Alcobaça Fm. share one species, with intraspecific variation, despite being derived from different ecosystems and from different ages (late Kimmeridgian to early Tithonian for the former; Kimmeridgian for the latter). Based on its features, it is here proposed that, at the very least, ML2738 (Figure 4A) could represent a juvenile. However, frontal bones in *albanerpetontids* appear to be plastic enough, at least at the specific level to be less diagnostic than previously thought. This may be significant in the case of the genus *Celtesdens*, as its diagnosis is based entirely on characters of the frontals (McGowan 1998; Gardner 2000a). Similar plasticity had also been reported in other diagnostic bones of *albanerpetontids* (Sweetman and Gardner 2013), which reinforces the need to consider this variation, to determine whether or not it reflects true intraspecific or interspecific variation. However, such distinction may prove problematic in the case of the fragmentary and isolated the material.

Phylogenetic position and systematic implications of the new material

The phylogeny presented in this study confirms the paraphyly observed in the genus *Albanerpeton* (Matsumoto and Evans 2018; Daza et al. 2020), which appears now to be invalid for a number of species as it is currently defined. However, due to the instability of the current phylogeny, revising the monophyly of *Albanerpeton* is beyond the scope of this paper and will be part of a further dedicated study of *Albanerpetontidae*. In summary, this preliminary analysis heightens the need for a complete revision for the phylogeny of the group: attribution of the Uña specimen to *Wesserpeton* is not supported, contradicting previous assessment (Sweetman and Gardner 2013) and suggesting the specimen needs a detailed

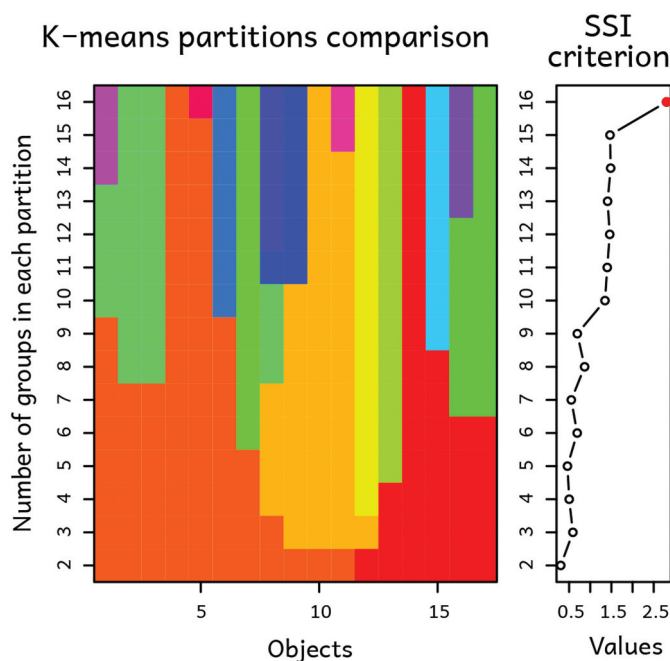


Figure 11. K-mean partitions comparison and the associated SSI criterion for up to 16 groups.

description; and the genus *Celtedens* collapsed into a basal polytomy of the group when characters relating to both species were included in the analysis.

The 9 characters relating to the frontal bones in our matrix were recovered in 20 character changes through the phylogeny (Figure 12, Supplementary file 6). The high degree of homoplasy and low homology observed in four of the frontal bone related characters (23, 24, 32 and 38), coupled with the general low support of the recovered tree, suggests that the synapomorphic condition of these character state transformations should be considered with caution.

Our results support the use of frontal bones to differentiate genera of Albanerpetontidae, but suggest they are not diagnostic at species level.

Portuguese specimens do indeed share the diagnostic characters of *Celtedens*: fused frontals bearing bulbous-shaped internasal process and retaining a bell-shaped outline; proportion of midline length to width across posterior edge between lateral edges of ventrolateral crests greater than 1.2; internasal process ventrolaterally has a facet for dorsally overlapping medial edge of nasal; dorsal and ventral edges of slot for receipt of prefrontal not excavated

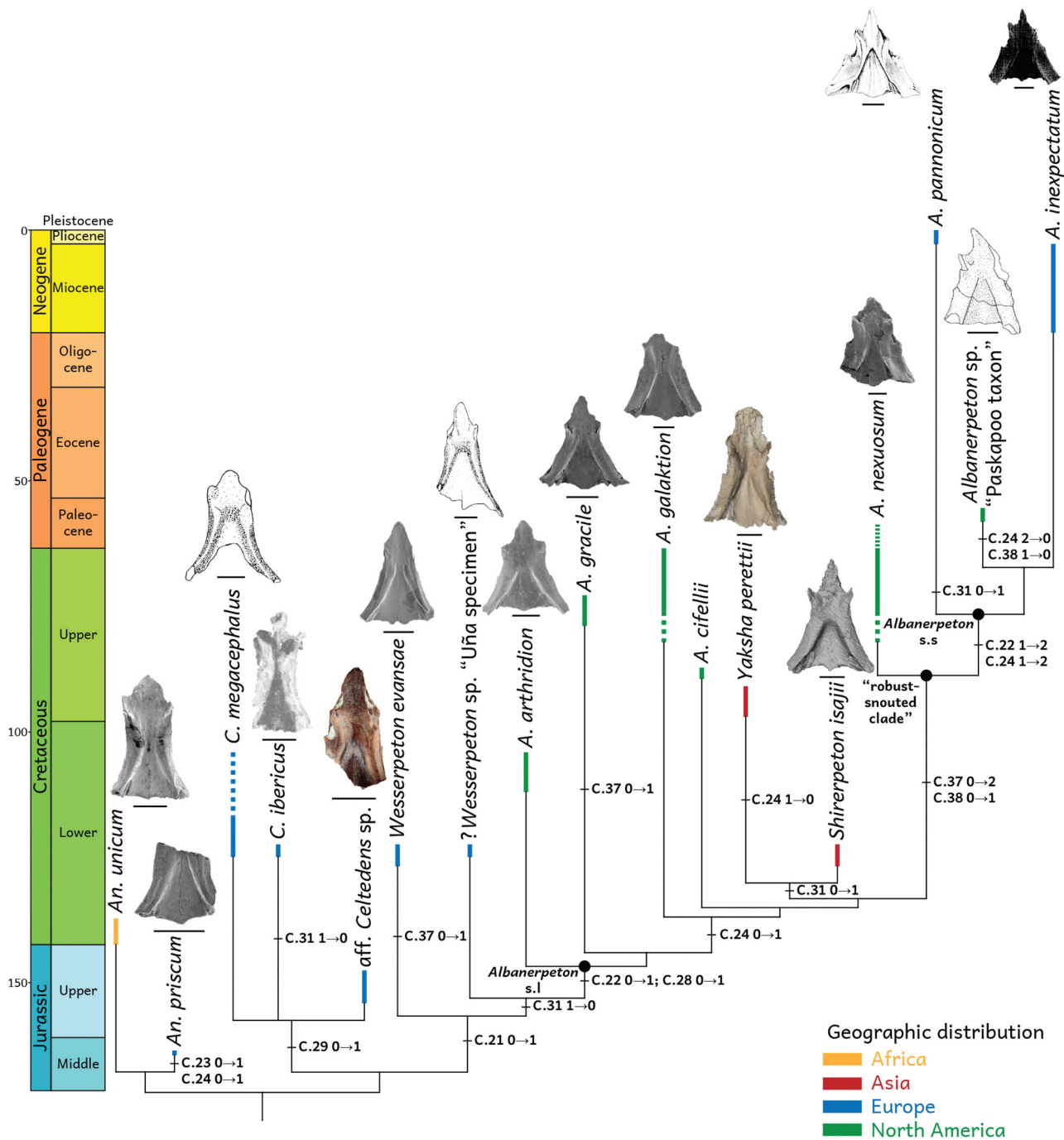


Figure 12. Evolution of the frontal bone in Albanerpetontidae, based on the consensus tree from the present analysis plotted against time and with geographic occurrences. Nodes are not time-calibrated. Frontals are from the literature and associated with their respective species (scale bars represent 1 mm). No frontal has been described yet for *Albanerpeton cifellii* (Gardner 1999c). Synapomorphies related to the frontal bones are indicated by lower-case letters.

medially; anterior end of orbital margin located anterior to anteroposterior midpoint of frontals; and orbital margin deeply concave in dorsal or ventral outline, occasionally deflected posterolaterally near posterior end (McGowan 1998; Gardner 2000a). However, the frontals do exhibit differentiated anterolateral processes. It could not be determined if the lacrimal facets are indented; hence their assignment to aff. *Celtedens* sp. They share 9 characters with *C. ibericus* and *C. megacephalus*, of which 8 are characters of the frontal, *Celtedens* being diagnosed on characters of the frontals alone (McGowan 1998; Gardner 2000a). Among those characters, aff. *Celtedens* sp. shares the diagnostic bulbous internasal process (char 29; 1). In the present analysis, this character is the only synapomorphy characterising *Celtedens*. Furthermore, *C. ibericus* and aff. *Celtedens* sp. share 14 additional characters and differ in two more. However, these 16 characters, unrelated to the frontals, are inconclusive, as they are not coded in *C. megacephalus*, despite being related to other bones that could provide insights concerning relationships among *Celtedens* species. The specimen from Pietraröia is poorly documented and preserved (Gardner 2000a; McGowan 2002; Maddin et al. 2013) with only 9 characters coded in this matrix (23.7%), among which 8 are related to the frontal bones. All these characters are those shared with the other *Celtedens* species. A complete revision of the Italian specimen, together with specimens from Las Hoyas, using modern digital techniques may yield a new and better diagnosis of the genus, as illustrated in recent works for Asian specimens (Matsumoto and Evans 2018; Daza et al. 2020).

Indeed, diagnoses of *C. megacephalus* and *C. ibericus* are only based on putative autapomorphies of the frontal bones (McGowan 1998): the curvature of the orbital margin and the relative proportion of the anterior inter-lacrimal width (slot width, between the posterior slots for the prefrontal SW in our measurements, Figure 3) to the posterior parietal margin width (frontal width across posterior edges FW in our measurements, Figure 3). In both characters, aff. *Celtedens* sp. is more similar to *C. megacephalus* than it is to *C. ibericus*. However, as seen in the morphometric analysis, both characters also present disparity in the Portuguese specimens and may be affected by ontogeny, which would question the validity of this character for the respective diagnoses. However, accurate measurements on specimens of both published species would be required to characterise this ratio, as it appears to be quite variable in our sample.

Conclusion

Sixty-two new frontals from the Lourinhã Formation are described, together with 58 revised specimens from the Guimarota beds, and are attributed to aff. *Celtedens* sp., based on their frontal bone morphology: a bell-shaped outline; and a flabellate, bulbous internasal process. This material confirms the plastic nature of the frontal bone, a key element in the characterisation of Albanerpetontidae. While frontal morphology can be used in isolation to discriminate some genera, it should not be used in isolation to diagnose species. Linear morphometric analysis paired with anatomical description highlights several features (notably the dorsal ornamentation, the shape and extent of the ventrolateral crests, the curvature of orbital margins, the size of the internasal process relative to the midline length of the frontals, the size of the slot width relative to the frontal width across posterior edges, and the presence of a ventromedian crest), that vary greatly from one specimen to another and, therefore, could affect taxonomic assessment, especially as some features are considered diagnostic in *Celtedens*. Preliminary phylogenetic analysis confirms the paraphyly of *Albanerpeton* s.l., and thus the need for nomenclatural revision of

most its species, as previously reported. Furthermore, our results confirm the validity of *Celtedens*, but suggest the need for a complete revision of the specimens referred to this genus. Finally, frontal bones show a high degree of homoplasy in details of their morphology, so characters based on this skeletal element should be carefully analysed before being regarded as diagnostic for a taxon.

Abbreviations

Institutional: FCT/UNL, Faculdade de Ciências e Tecnologia – Universidade Nova de Lisboa; IPFUB, Institute of Geological Sciences, Freie Universität Berlin; MG, Museu Geológico (Lisboa); ML, Museu da Lourinhã; PDL, Parque dos Dinossauros de Lourinhã.

Anatomical: **Ap**, anterolateral process; **Ca**, canal; **Fo**, foramen; **Ip**, internasal process; **Lif**, lateroventral internasal facet; **Mpf**, middle part of the frontal; **Naf**, nasal facet; **Om**, orbital margin; **Pf**, parietal facet; **Pff**, prefrontal facet; **Vc**, ventrolateral crest; **Vr**, ventral roof; **Vs**, ventromedian suture.

Measurements: **CPE**, curvature at the posterior part of the edge (in degrees); **FIW**, frontal inner width between ventrolateral crests, across posterior edges of the frontal ventral roof; **FL**, total length of the frontal; **FML**, frontal length at the midline; **FW**, frontal width across posterior edges; **INL**, internasal length at the midline; **INW**, internasal width at the base; **IVCW**, interventrolateral crests width; **OML**, orbital margin length; **SW**, slot width between the posterior slots for the prefrontal; **VCAW**, ventrolateral crest anterior width, behind prefrontal facets; **VCC**, ventrolateral crest curvature (in degrees); **VCPW**, ventrolateral crest posterior width, before parietal facets.

Acknowledgments

We thank the municipality of Lourinhã for providing the 'Espaço NovaPaleo' to work. We want to give special thanks to André Saleiro, who helped to prepare and pick the residues, Micael Martinho and Alexandra Fernandes for their tremendous contribution in picking and finding the best-preserved specimens, and to Jorge Sequeira and Museu Geológico in Lisbon for providing access to the Guimarota collection. Peterson Lopes (Universidade do Sa Paulo, Brasil) wrote the statsall.run script for TNT. We are grateful for the Master students from FCT-UNL and all volunteers who participated in the MicroSaurus Citizen Science Project hosted by the DinoPark of Lourinhã (PDL). We thank the comments of the three reviewers and the editor Gareth Dyke, who greatly improved our original draft.

Authors contribution

Conceptualization – ARDG, MMA, OM
 Formal analysis – ARDG, MMA
 Investigation – ARDG, CN, MMA, OM
 Methodology – ARDG, CN, MMA, OM
 Supervision – MMA, OM
 Writing – original draft – ARDG, MMA
 Writing – review & edit – ARDG, CN, MMA, OM

Data availability statement

Data for this study including the NEXUS files are available in MorphoBank (project 4114): https://morphobank.org/index.php/Projects/ProjectOverview/project_id/4114 [please note that the data for this paper are not yet published and this temporary link should not be shared without the express permission of the author]

Disclosure statement

No potential conflict of interest was reported by the author(s).

Funding

This work was supported by the Fundação para a Ciência e Tecnologia (FCT-MCTES) of Portugal under Grants PTDC/CTA-PAL/31656/2017, PTDC/CTA-PAL/2217/2021, and UIDB/04035/2020; and by PDL under research Grant Parque dos Dinossauros de Lourinhã Microsaurus-superanimais 3. ARDG is supported by FCT-MCTES, grant number SFRH/BD/144665/2019.

ORCID

Alexandre R. D. Guillaume  <http://orcid.org/0000-0002-9005-9916>
 Octávio Mateus  <http://orcid.org/0000-0003-1253-3616>
 Miguel Moreno-Azanza  <http://orcid.org/0000-0002-7210-1033>

References

- Alves T, Manuppella G, Gawthorpe R, Hunt D, Monteiro J. 2003. The depositional evolution of diapir- and fault-bounded rift basins: examples from the Lusitanian Basin of West Iberia. *Sedimentary Geology*. 162(3–4):273–303. doi:10.1016/S0037-0738(03)00155-6.
- Anderson JS. 2008. Focal review: The Origin(s) of Modern Amphibians. *Evol Biol*. 35(4):231–247. doi:10.1007/s11692-008-9044-5.
- Borcard D, Gillet F, Legendre P. 2018. *Numerical Ecology with R*. 2nd ed. New York City (NY): Springer.
- Carrano MT, Oreska MPJ, Murch A, Trujillo KC, Chamberlain KR. 2022. Vertebrate paleontology of the Cloverly Formation (Lower Cretaceous), III: a new species of *Albanerpeton*, with biogeographic and paleoecological implications. *Journal of Vertebrate Paleontology*. e2003372. doi:10.1080/02724634.2021.2003372
- Costa OG. 1864. Paleontologia del Regno di Napoli. Part III. *Atti dell'Accademia Pontaniana*. 8:1–128.
- Daza JD, Stanley EL, Bolet A, Bauer AM, Arias JS, Čerňanský A, Bevitt JJ, Wagner P, Evans SE. 2020. Enigmatic amphibians in mid-Cretaceous amber were chameleon-like ballistic feeders. *Science*. 370(6517):687–691. doi:10.1126/science.abb6005.
- Estes R. 1981. *Gymnophiona*, Caudata. In: Wellnhofer P, editor. *Encyclopedia of Paleoherpology*. Gustav Fischer Verlag. Stuttgart; p. 1–115.
- Estes R, Hoffstetter R. 1976. Les Urodèles du Miocène de La Grive-Saint-Alban (Isère, France). *Bulletin du Muséum national d'Histoire naturelle*, 3e série. 398:297–343.
- Evans SE. 2016. *Albanerpetontidae*. In: Poyato-Ariza FJ, Buscalioni AD, editors. *Las Hoyas: a Cretaceous wetland*. Munich: Verlag Dr. Friedrich Pfeil; p. 133–137.
- Evans SE, Milner AR. 1994. Middle Jurassic microvertebrate assemblages from the British Isles. In: Fraser NC, Evans SE, editors. *In the shadow of the dinosaurs: Early Mesozoic Tetrapods*. Cambridge: Cambridge University Press; p. 303–321.
- Fox RC, Naylor BG. 1982. A reconsideration of the relationships of the fossil amphibian *Albanerpeton*. *Canadian Journal of Earth Sciences*. 19(1):118–128. doi:10.1139/e82-009.
- Gardner JD. 1999a. The amphibian *Albanerpeton arthridion* and the Aptian–Albian biogeography of albanerpetontids. *Palaeontology*. 42(3):529–544. doi:10.1111/1475-4983.00083.
- Gardner JD. 1999b. Redescription of the geologically youngest albanerpetontid (? Lissamphibia): *Albanerpeton inexpectatum* Estes and Hoffstetter, 1976, from the Miocene of France. *Annales de Paléontologie*. 85(1):57–84. doi:10.1016/S0753-3969(99)80008-1.
- Gardner JD. 1999c. New albanerpetontid amphibians from the Albian to Coniacian of Utah, USA—bridging the gap. *Journal of Vertebrate Paleontology*. 19(4):632–638. doi:10.1080/02724634.1999.10011177.
- Gardner JD. 2000a. Revised taxonomy of albanerpetontid amphibians. *Acta Palaeontologica Polonica*. 45(1):55–70.
- Gardner JD. 2000b. Albanerpetontid amphibians from the Upper Cretaceous (Campanian and Maastrichtian) of North America. *Geodiversitas*. 22(3):349–388.
- Gardner JD. 2001. Monophyly and affinities of albanerpetontid amphibians (Temnospondyli; Lissamphibia). *Zoological Journal of the Linnean Society*. 131(3):309–352. doi:10.1111/j.1096-3642.2001.tb02240.x.
- Gardner JD. 2002. Monophyly and intra-generic relationships of *Albanerpeton* (Lissamphibia; Albanerpetontidae). *Journal of Vertebrate Paleontology*. 22(1):12–22. doi:10.1671/0272-4634(2002)022[0012:MAIGRO]2.0.CO;2.
- Gardner JD, Böhme M. 2008. Review of the Albanerpetontidae (Lissamphibia), with Comments on the Paleocological Preferences of European Tertiary Albanerpetontids. In: Sankey JT, Bazio S, editors. *Vertebrate Microfossil Assemblages: Their Role in Paleocology and Paleobiogeography*. Bloomington: Indiana University Press; p. 178–218.
- Gardner JD, Evans SE, Sigogneau-Russel D. 2003. New albanerpetontid amphibians from the Early Cretaceous of Morocco and Middle Jurassic of England. *Acta Palaeontologica Polonica*. 48(2):301–319.
- Gardner JD, Villa A, Colombero S, Venczel M, Delfino M. 2021. A Messinian (latest Miocene) occurrence for *Albanerpeton* Estes & Hoffstetter, 1976 (Lissamphibia: Albanerpetontidae) at Moncucco Torinese, Piedmont Basin, northwestern Italy, and a review of the European Cenozoic record for albanerpetontids. *Geodiversitas*. 43(14):391–404. doi:10.5252/geodiversitas2021v43a14.
- Gloy U. 2000. Taphonomy of the fossil lagerstätte Guimarota. In: Martin T, Krebs B, editors. *Guimarota: a Jurassic ecosystem*. Munich: Verlag Dr. Friedrich Pfeil; p. 129–136.
- Goloboff PA, Catalano SA. 2016. TNT version 1.5, including a full implementation of phylogenetic morphometrics. *Cladistics*. 32(3):221–238. doi:10.1111/cla.12160.
- Goloboff PA, Farris JS, Nixon KC. 2008. TNT, a free program for phylogenetic analysis. *Cladistics*. 24(5):774–786. doi:10.1111/j.1096-0031.2008.00217.x.
- Gowland S, Taylor AM, Martinus AW. 2017. Integrated sedimentology and ichnology of Late Jurassic fluvial point bars—facies architecture and colonization styles (Lourinhã Formation, Lusitanian Basin, western Portugal). *Sedimentology*. p. 1–31. doi:10.1111/sed.12385.
- Guillaume ARD, Moreno-Azanza M, Puértolas-Pascual E, Mateus O. 2020. Palaeobiodiversity of crocodylomorphs from the Lourinhã Formation based on the tooth record: insights into the palaeoecology of the Late Jurassic of Portugal. *Zoological Journal of the Linnean Society*. 189(2):549–583. doi:10.1093/zoolin/zl112.
- Haddoumi H, Allain R, Meslouh S, Metais G, Monbaron M, Pons D, Rage J-C, Vullo R, Zouhri S, Gheerbrant E. 2016. Guelb el Ahmar (Bathonian, Anoual Syncline, eastern Morocco): first continental flora and fauna including mammals from the Middle Jurassic of Africa. *Gondwana Research*. 29(1):290–319. doi:10.1016/j.jr.2014.12.004.
- Haeckel E. 1866. *Generelle Morphologie der Organismen allgemeine Grundzüge der organischen Formen-Wissenschaft, mechanisch begründet durch die von Charles Darwin reformirte Descendenz-Theorie von Ernst Haeckel: allgemeine Entwicklungsgeschichte der Organismen kritische G*. Berlin: Verlag von Georg Reimer.
- Hahn G, Hahn R. 2001. Multituberculaten-Zähne aus dem Ober-Jura von Porto das Barcas (Portugal). *Paläontologische Zeitschrift*. 74(4):583–586. doi:10.1007/BF02988164.
- Hammer Ø, Harper DA, Ryan PD. 2001. PAST: paleontological statistics software package for education and data analysis. *Palaeontologia Electronica*. 4(1):9.
- Helmdach FF. 1971. Stratigraphy and ostracod-fauna from the coalmine Guimarota (Upper Jurassic). *Contribuição para o conhecimento da fauna do Kimeridgiano da mina de lignito Guimarota (Leiria, Portugal) II Parte: IV. Memórias dos Serviços geológicos de Portugal*. 17:41–88.
- Jackson DA. 1993. Stopping rules in principal components analysis: a comparison of heuristic and statistical approaches. *Ecology*. 74(8):2204–2214. doi:10.2307/1939574.
- Krebs B. 2000. The excavations in the Guimarota mine. In: Martin T, Krebs B, editors. *Guimarota: a Jurassic ecosystem*. Munich: Verlag Dr. Friedrich Pfeil; p. 9–20.
- Lasseron M, Allain R, Gheerbrant E, Haddoumi H, Jalil N-E, Métais G, Rage J-C, Vullo R, Zouhri S. 2020. New data on the microvertebrate fauna from the Upper Jurassic or lowest Cretaceous of Ksar Metlili (Anoual Syncline, eastern Morocco). *Geological Magazine*. 157(3):367–392. doi:10.1017/S0016756819000761.
- Leinfelder RR, Wilson RC. 1989. Seismic and sedimentologic features of Oxfordian–Kimmeridgian syn-rift sediments on the eastern margin of the Lusitanian Basin. *Geologische Rundschau*. 78(1):81–104. doi:10.1007/BF01988355.
- Linnaeus C. 1758. *Systema naturae, sive regna tria naturae systematice proposita per classes, ordines, genera, & species*. 10th ed. Leiden: Haak.
- Maddin HC, Venczel M, Gardner JD, Rage J-C. 2013. Micro-computed tomography study of a three-dimensionally preserved neurocranium of *Albanerpeton* (Lissamphibia, Albanerpetontidae) from the Pliocene of Hungary. *Journal of Vertebrate Paleontology*. 33(3):568–587. doi:10.1080/02724634.2013.722899.
- Maddison WP, Maddison DR. 2019. Mesquite: a modular system for evolutionary analysis [Internet]. [place unknown]. <http://www.mesquiteproject.org>
- Marjanović D, Laurin M. 2008. A reevaluation of the evidence supporting an unorthodox hypothesis on the origin of extant amphibians. *Contributions to Zoology*. 77(3):149–199. doi:10.1163/18759866-07703002.
- Marjanović D, Laurin M. 2019. Phylogeny of paleozoic limbed vertebrates reassessed through revision and expansion of the largest published relevant data matrix. *PeerJ*. 6:e5565. doi:10.7717/peerj.5565
- Martin T. 2000. Overview over the Guimarota ecosystem. In: Martin T, Krebs B, editors. *Guimarota A Jurassic ecosystem*. Munich: Verlag Dr. Friedrich Pfeil; p. 143–146.
- Martin T. 2001. Mammalian fauna of the Late Jurassic Guimarota ecosystem. *Publicación Electrónica de la Asociación Paleontológica Argentina*. 7(1):123–126.
- Martinus AW, Gowland S. 2011. Tide-influenced fluvial bedforms and tidal bore deposits (Late Jurassic Lourinhã Formation, Lusitanian Basin, Western Portugal). *Sedimentology*. 58(1):285–324. doi:10.1111/j.1365-3091.2010.01185.x.

- Mateus O, Dinis J, Cunha P. 2017. The Lourinhã Formation: the Upper Jurassic to lowermost Cretaceous of the Lusitanian Basin, Portugal – landscapes where dinosaurs walked. *Ciências da Terra - Earth Sciences Journal*. 19 (1):75–97. doi:10.21695/cterra/esj.v19i1.355.
- Matsumoto R, Evans SE, Smith T. 2018. The first record of albanerpetontid amphibians (Amphibia: Albanerpetontidae) from East Asia. *PLoS one*. 13(1): e0189767. doi:10.1371/journal.pone.0189767.
- McGowan GJ. 1998. Frontals as diagnostic indicators in fossil albanerpetontid amphibians. *Bulletin of the National Science Museum, Series C (Geology and Paleontology)*. 24:185–194.
- McGowan GJ. 2002. Albanerpetontid amphibians from the Lower Cretaceous of Spain and Italy: a description and reconsideration of their systematics. *Zoological Journal of the Linnean Society*. 135(1):1–32. doi:10.1046/j.1096-3642.2002.00013.x.
- McGowan G, Evans S. 1995. Albanerpetontid amphibians from the Cretaceous of Spain. *Nature*. 373(6510):143–145. doi:10.1038/373143a0.
- Oksanen J, Blancher FG, Friendly M, Kindt R, Legendre P, McGlinn D, Minchin PR, O'Hara RB, Simpson GL, Solymos P, et al. 2020. *vegan*: Community Ecology Package. <https://cran.r-project.org>, <https://github.com/vegandevs/vegan>
- Rasband WS. 2003 *Image J*. National Institutes of Health, Bethesda, Maryland, USA. <http://rsb.info.nih.gov/ij/>
- Ribeiro A, Antunes MT, Ferreira MP, Rocha RB, Soares AF, Zbyszewski G, De Almeida FM, De Carvalho D, Monteiro JH. 1979. *Introduction à la géologie générale du Portugal*. Lisboa: Serviços geológicos de Portugal.
- Schudack ME. 2000a. Geological setting and dating of the Guimarães beds. In: Martin T, Krebs B, editors. *Guimarães: a Jurassic ecosystem*. Munich: Verlag Dr. Friedrich Pfeil; p. 21–26.
- Schudack ME. 2000b. Ostracodes and charophytes from the Guimarães beds. In: Martin T, Krebs B, editors. *Guimarães: a Jurassic ecosystem*. Munich: Verlag Dr. Friedrich Pfeil; p. 33–36.
- Schudack ME, Turner CE, Peterson F. 1998. Biostratigraphy, paleoecology and biogeography of charophytes and ostracodes from the Upper Jurassic Morrison Formation, Western Interior, USA. *Modern Geology*. 22(1):379–414.
- Seiffert J. 1969. Urodelen-atlas aus dem obersten Bajocien von SE-Aveyron (Südfrankreich). *Paläontologische Zeitschrift*. 43(1–2):32–36. doi:10.1007/BF02987925.
- Skutschas PP. 2007. New specimens of albanerpetontid amphibians from the Upper Cretaceous of Uzbekistan. *Acta Palaeontologica Polonica*. 52 (4): 819–821.
- Sweetman SC, Gardner JD. 2013. A new albanerpetontid amphibian from the Barremian (Early Cretaceous) Wessex Formation of the Isle of Wight, southern England. *Acta Palaeontologica Polonica*. 58(2):295–324.
- Taylor AM, Gowland S, Leary S, Keogh KJ, Martinius AW. 2014. Stratigraphical correlation of the Late Jurassic Lourinhã Formation in the Consolação Sub-basin (Lusitanian Basin, Portugal). *Geological Journal*. 49(2):143–162. doi:10.1002/gj.2505.
- Venczel M, Gardner JD. 2005. The geologically youngest albanerpetontid amphibian, from the lower Pliocene of Hungary. *Palaeontology*. 48 (6):1273–1300. doi:10.1111/j.1475-4983.2005.00512.x.
- Villa A, Blain H-A, Delfino M. 2018. The Early Pleistocene herpetofauna of Rivoli Veronese (Northern Italy) as evidence for humid and forested glacial phases in the Gelasian of Southern Alps. *Palaeogeography, Palaeoclimatology, Palaeoecology*. 490:393–403. doi:10.1016/j.palaeo.2017.11.016
- Wickham H, Chang W, Henry L, Pedersen TL, Takahashi K, Wilke C, Woo K, Yutani H, Dunnington D. 2021. *ggplot2: Create elegant data visualisations using the grammar of graphics*. <https://cloud.r-project.org/web/packages/ggplot2/index.html>
- Wiechmann MF. 2000. The albanerpetontids from the Guimarães mine. In: Martin T, Krebs B, editors. *Guimarães: a Jurassic ecosystem*. Munich: Verlag Dr. Friedrich Pfeil; p. 51–54.
- Wiechmann MF. 2003. *Albanerpetontidae (Lissamphibia) aus dem Mesozoikum der Iberischen Halbinsel und dem Neogen von Süddeutschland* [PhD dissertation]. Berlin: Freie Universität Berlin.
- Wilson RC, Hiscott RN, Willis MG, Gradstein FM. 1989. The Lusitanian Basin of West-Central Portugal: Mesozoic and Tertiary tectonic, stratigraphic, and subsidence history. In: AJ Tankard, HL Balkwill, editors. *Extensional tectonics and stratigraphy of the North Atlantic margins AAPG memoir 46: american association of Petroleum Geologists*. Vol. 46. Calgary (AB): Canadian Geological Foundation; p. 341–361.